European Journal of Medicinal Chemistry 220 (2021) 113449

Contents lists available at ScienceDirect

European Journal of Medicinal Chemistry

journal homepage: http://www.elsevier.com/locate/ejmech

Discovery of highly potent tubulin polymerization inhibitors: Design, synthesis, and structure-activity relationships of novel 2,7-diaryl-[1,2,4]triazolo[1,5-*a*]pyrimidines

Xian-Sen Huo [1], Xie-Er Jian [1], Jie Ou-Yang [1], Lin Chen, Fang Yang, Dong-Xin Lv, Wen-Wei You, Jin-Jun Rao**, Pei-Liang Zhao*

Guangdong Provincial Key Laboratory of New Drug Screening, School of Pharmaceutical Science, Southern Medical University, Guangzhou, 510515, PR China

ARTICLE INFO

Article history:
Received 16 December 2020
Received in revised form
3 April 2021
Accepted 4 April 2021
Available online 16 April 2021

Keywords:
2,7-Diaryl-[1,2,4]triazolo[1,5-*a*]pyrimidine
Anticancer agents
Tubulin inhibitors

ABSTRACT

By removing 5-methyl and 6-acetyl groups in our previously reported compound **3**, we designed a series of novel 2,7-diaryl-[1,2,4]triazolo[1,5-*a*]pyrimidine derivatives as potential tubulin polymerization inhibitors. Among them, compound **5e** displayed low nanomolar antiproliferative efficacy on HeLa cells which was 166-fold higher than the lead analogue **3**. Interestingly, **5e** displayed significant selectivity in inhibiting cancer cells over HEK-293 (normal human embryonic kidney cells). In addition, **5e** dose-dependently arrested HeLa in G2/M phase through the alterations of the expression levels of p-cdc2 and cyclin B1, and caused HeLa cells apoptosis by regulation of expressions of cleaved PARP. Further evidence demonstrated that **5e** effectively inhibited tubulin polymerization and was 3-fold more powerful than positive control CA-4. Moreover, molecular docking analysis indicated that **5e** overlapped well with CA-4 in the colchicine-binding site. These studies demonstrated that 2,7-diaryl-[1,2,4]triazolo [1,5-*a*]pyrimidine skeleton might be used as the leading unit to develop novel tubulin polymerization inhibitors as potential anticancer agents.

1. Introduction

Microtubules are highly dynamic frameworks composed by α- and β-tubulin dimmers, which are involved in abundant fundamental cellular processes, including maintenance of cytoskeleton, cell division, spindle formation and intracellular trafficking [1]. These aforementioned vital roles make tubulin an extremely attractive target for clinically effective anticancer drugs [2–5].

In last decades, great deals of chemically diverse natural and synthetic compounds targeting tubulin have been explored [6–10], among which, a natural *cis*-stilbene derivative CA-4 (Fig. 2) presents strong antiproliferative activities toward multiple cancer cell lines, including cells bearing a multidrug resistance phenotype, and inhibits tubulin polymerization through interacting with tubulin at the colchicine binding site [11]. However, CA-4 possessed poor activity *in vivo* because of poor water solubility and low bioavailability, and its phosphate disodium CA-4P is under evaluation in phase III trials for the treatment of anaplastic thyroid cancer and other advanced solid tumors [12,13]. Hence, CA-4 has always been considered as a promising lead compound as a tubulin polymerization inhibitor since its discovery, and extensive investigations strongly demonstrated that the *cis*-configuration of the olefinic double bond is essential for antiproliferative activity, and fixing this bond through incorporation into heterocycle rings has recently become a well-verified strategy [14–18]. In addition [1,2,4]triazolo[1,5-*a*]pyrimidine scaffold is highly privileged in medicinal chemistry due to its versatile pharmacological activity profile, such as anticancer [19,20], antimicrobial [21], antiviral [22], herbicidal [23–26], and fungicidal activities [27]. Our research group has explored a great number of fused bicyclic systems as *cis*-restricted CA-4 analogues [28–33], and more recently we also reported a series of 6-acetyl-5-methyl- [1,2,4]triazolo[1,5-*a*]pyrimidine derivatives as new tubulin inhibitors, exampled by analogue **3** which showed potent antiproliferative properties in inducing G2/M arrest and remarkable antitubulin activity [28]. The potent antitumor activity made the class of compounds worth further evaluation.

* Corresponding author.
** Corresponding author.
E-mail addresses: raojj@smu.edu.cn (J.-J. Rao), plzhao@smu.edu.cn (P.-L. Zhao).
[1] Authors contributed equally to this work.

https://doi.org/10.1016/j.ejmech.2021.113449
0223-5234/

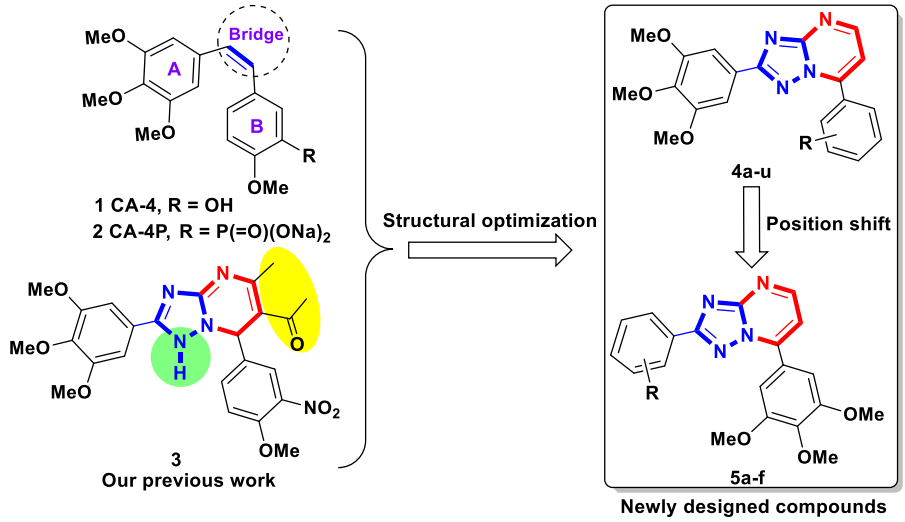

Fig. 1. Structures of several reported tubulin inhibitors **1**–**3**, and newly designed compounds **4a**–**u** and **5a**–**f**.

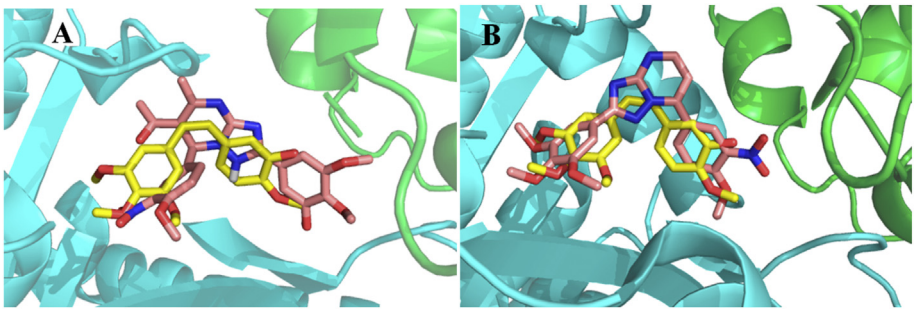

Fig. 2. Predicted binding mode of (**A**) **3** (amber stick) and (**B**) corresponding **4** (amber stick) with tubulin (PDB code: 5lyj) and overlapping with CA-4 (yellow stick).

Our previous docking studies indicated that 5-methyl and 6-acetyl groups of the triazolopyrimidine core would be more sterically restrictive of the molecule in the binding pocket. The modeling studies further revealed that both compound **3** and corresponding **4** without two substituents could dock within the tubulin–colchicine binding site. But 3,4,5-trimethoxyphenyl of compound **3** can't overlap with that of CA-4, while analogue **4** superimposed well with CA-4 (Fig. 2). Hence, in our current study, a series of new [1,2,4]triazolo[1,5-*a*]pyrimidine derivatives **4a**–**u** were designed by removing 5-methyl and 6-acetyl groups in compound **3**. Meanwhile**,** we shifted 3,4,5-trimethoxyphenyl from C-2 to C-7 position to attain the derivatives with typical structure **5a**–**f** (Fig. 1). To the best of our knowledge, these target compounds were unexplored so far as tubulin polymerization inhibitors.

2. Chemistry

Synthesis of newly designed 2,7-diaryl- [1,2,4]triazolo[1,5-*a*] pyrimidine analogues **4a**–**u** and **5a**–**f** was outlined in Scheme 1. The key intermediates 3-substituted 5-amino-1,2,4-triazoles **9** and **16** for the final cyclization reaction were obtained in four steps starting with appropriate benzoic acids according to reported procedure [34]. Meanwhile, commercially available ketones **10** and **17** were reacted with an excess of *N,N*-dimethylformamide dimethyl acetal (DMFDMA) under solvent-free conditions at 90 °C to give arylpropenones **12** with good yields [33,34], which were then condensed with 5-amino-1,2,4-triazoles **9** and **16** in EtOH or AcOH at reflux to generate the required products **4a**–**u** and **5a**–**f** in yields ranging from 52 to 84%. All final analogues were fully characterized through various spectroscopic techniques including ^{1}H NMR, ^{13}C NMR, and HRMS, which were provided in the Experimental Section.

3. Results and discussion

3.1. In vitro cell growth inhibitory activity

The *in vitro* cell growth inhibitory activity of 27 newly synthesized derivatives **4a**–**u** and **5a**–**f** were first screened toward HeLa (human cervical cancer cell line) by the conventional MTT assay with our previously reported compound **3** and CA-4 as positive controls. The results were illustrated in Table 1.

In general, almost all investigated compounds **4a**–**u** (except for **4g**, **4m**, **4p** and **4r**) having 3,4,5-trimethoxyphenyl group in position 2 of triazolopyrimidine ring, didn't display potent antiproliferative efficacy toward HeLa possessing IC_{50} values higher than 30 μM. Notably, among these compounds, **4m** with the 3-amino-4-methoxyphenyl substituent showed the highest cytotoxicity with an IC_{50} value of 0.40 μM. Interestingly, most corresponding compounds **5a**–**f** bearing 3,4,5-trimethoxyphenyl in position 7 of the fused core displayed excellent antitumor activities with IC_{50} values of nanomolar range, which revealed that the position of 3,4,5-trimethoxyphenyl group played a crucial role in antiproliferative activity. Within series of **5a**–**f**, compounds with

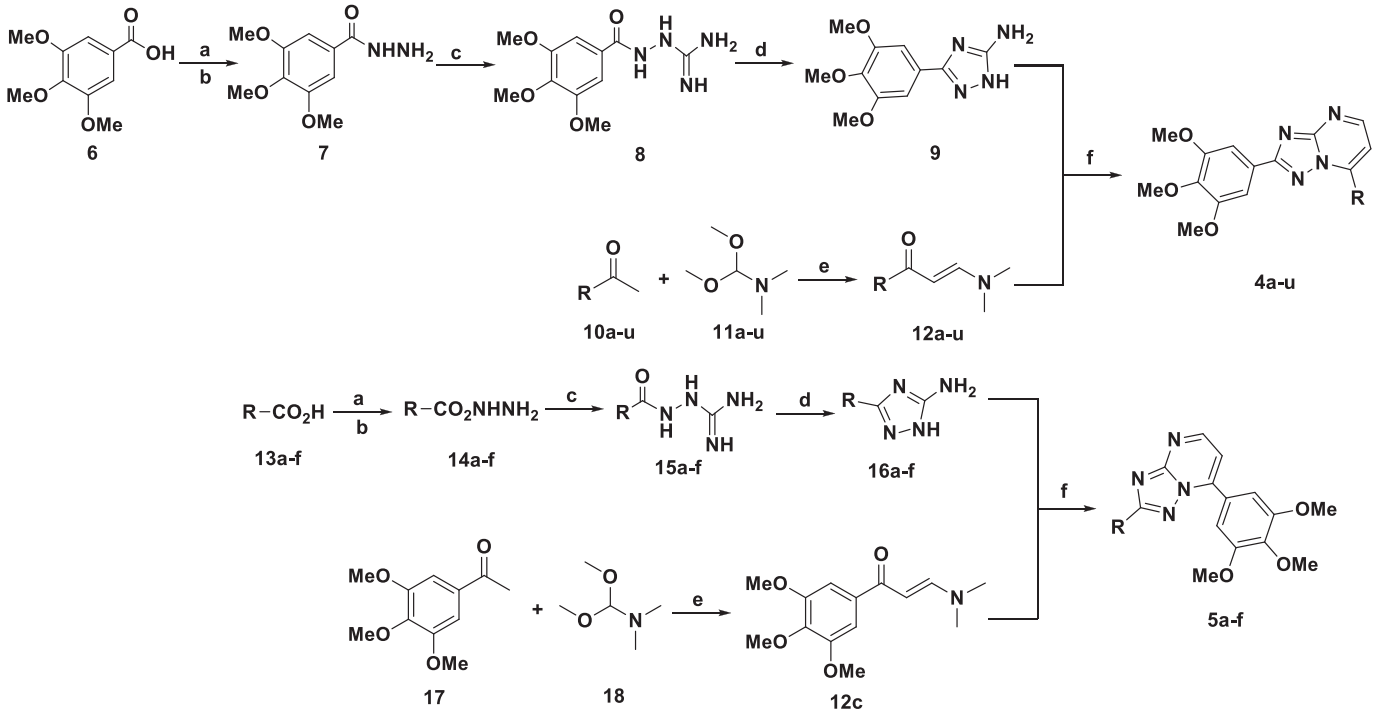

Scheme 1. Synthesis of 2,7-diaryl- [1,2,4]triazolo[1,5-*a*]pyrimidines **4a**–**u** and **5a**–**f**. Reagents and conditions: (a) conc. H_2SO_4, ethanol, reflux; (b) $NH_2NH_2 \cdot H_2O$, ethanol, reflux; (c) S-methylisothiourea sulfate; (d) 5% NaOH, 36 h, reflux; (e) 90 °C.; (f) AcOH, 80 °C; or EtOH, HCl, 80 °C.

Table 1
Growth inhibitory effects of compounds 4a–u and 5a–f toward HeLa cell line.

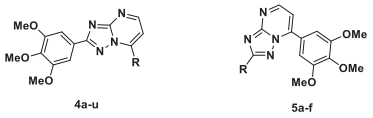

Compd.	R	IC_{50} mean ± SD[a] (μM)	Compd.	R	IC_{50} mean ± SD[a] (μM)
4a	3,4-$(CH_3O)_2$Ph	>30	**4p**	4-NH_2Ph	29.94 ± 2.80
4b	4-CH_3Ph	>30	**4q**		>30
4c	3,4,5-$(CH_3O)_3$Ph	>30	**4r**		28.56 ± 3.36
4d	4-CF_3Ph	>30	**4s**		>30
4e	3-F-4-CH_3OPh	>30	**4t**		>30
4f	2-CH_3Ph	>30	**4u**		>30
4g	4-CH_3CONHPh	22.16 ± 3.28	**5a**	3,4-Cl_2Ph	>30
4h	4-CO_2CH_3Ph	>30	**5b**	4-CH_3OPh	0.90 ± 0.02
4i	3-NO_2-4-CH_3OPh	>30	**5c**	4-CH_3Ph	>30
4j	4-CH_3OPh	>30	**5d**	3-NH_2-4-CH_3OPh	0.11 ± 0.01
4k	3,4-Cl_2Ph	>30	**5e**	3-HO-4-CH_3OPh	0.06 ± 0.01
4l	3-Cl-4-CH_3OPh	>30	**5f**	3-CH_3CONH-4-CH_3OPh	0.28 ± 0.04
4m	3-NH_2-4-CH_3OPh	0.40 ± 0.03	**3**	\	9.96 ± 0.05
4n	3,5-Cl_2-4- CH_3CONHPh	>30	**CA-4**	\	0.005 ± 0.0002
4o	4-NO_2Ph	>30			

[a] SD: standard deviation of three independent experiments.

electron-donating groups displayed much higher cytotoxicity than those having electron-withdrawing groups (**5b** vs. **5a**, **5d** vs. **5a**, **5e** vs. **5a**, **5f** vs. **5a**), which suggested that the introduction of electron-donating groups at phenyl ring of position 2 in triazolopyrimidine scaffold is more favorable for the antiproliferative potency. Particularly, in agreement with CA-4, analogue **5e** featuring 3-hydroxy-4-methoxyphenyl moiety, was found to be the most potent having the IC_{50} value of 60 nM and was about 166-fold more than that of the lead analogue **3** (IC_{50} = 9.96 μM). These results indicated that 2,7-diaryl- [1,2,4]triazolo[1,5-*a*]pyrimidine scaffold could be used as the leading unit to develop anticancer agents.

Next, some highly active analogues possessing excellent activity toward HeLa were chosen to further explore their antiproliferative activity profile on three another cancer types, such as human colon cancer cell line HCT116, human lung adenocarcinoma cell line A549, and human hepatoma cells HepG2, and the normal human embryonic kidney cell line (HEK-293). CA-4 was also utilized as a positive control. As depicted in Table 2, the results suggested that these derivatives revealed meaningful growth inhibitory activity on diverse cancer types. Particularly, **5e** displayed potent activities against A549, HepG2, and HCT116 with IC_{50} values of 6.05, 14.69, and 18.43 μM, respectively. Interestingly, **5e** exhibited no obvious cytotoxic activity (IC_{50} > 100 μM) toward HEK-293, whereas CA-4 demonstrated noticeable cytotoxity activity with the IC_{50} value of 45.69 μM. These findings manifested that **5e** could have significant selectivity on normal human cells.

3.2. HeLa cell cycle arrest and G2/M-related proteins regulation

To explore potential antitumor mechanism of this series of analogues, the most promising compound **5e** was selected to investigate for its effect on cell cycle progression of HeLa cells using flow cytometry analysis. In this work, Hela cells were treated with 30, 60 and 120 nM concentration of **5e** for 24 h, respectively. As depicted in Fig. 3, treatment with indicated concentrations of **5e,** percentages of cells at the G2/M phase of the cell cycle were increased from 16.18 to 46.82%, with respect to the control (12.49%). The results indicated that analogue **5e** concentration-dependently caused a significant G2/M arrest, which was a representative characteristic for tubulin polymerization inhibitors.

It is well known that mitosis-promoting factor generated between cell cycle regulatory proteins cyclin B1 and cdc2 acts as a crucial role in G2−M phase transition. Hence, it was considered of interest to study alterations of these proteins expression in order to gain insight in the mechanism involved in **5e**-induced G2/M arrest. The results shown in Fig. 4 indicated that **5e** concentration-dependently upregulated cyclin B1 protein level and significantly decreased expression of cdc2 protein, which suggested that G2/M-phase arrest induced by **5e** might be associated with regulation of expressions of p-cdc2 and cyclin B1.

3.3. HeLa cell apoptosis and caspase-3 activation

Subsequently, an Annexin V-FITC/PI assay was used to identify the cell apoptosis analysis of HeLa cells. As demonstrated in Fig. 5, after treatment with **5e** at the concentrations of 30, 60, and 120 nM, percentages of total apoptotic cells from 3.6% (control) increased to 14.1% (30 nM), 19.4% (60 nM), and 33.6% (120 nM), respectively. Hence, the results revealed that analogue **5e** possibly possessed the anti-proliferative effect through dose-dependently inducing of cellular apoptosis.

To explore the correlation between antiproliferative efficacy and cellular apoptosis, we investigated the cleavage of poly(ADP-ribose) polymerase (PARP) which is one of the important caspase-3-mediated cleavage targets in apoptosis induction. Additionally, Bax which is a key pro-apoptotic family protein was also observed. As shown in Fig. 6 in HeLa cells, **5e** induced a concentration-dependent increase in the expression of cleaved PARP after 24 h of treatment (30, 60 and 120 nM), which revealed that **5e** caused cancer cells apoptosis through activation of caspase-3. Whereas, there is no obvious change in the expression level of the Bax after treatment for 24 h. These findings indicated that analogue **5e** caused cell apoptosis through regulating expression of cleaved PARP.

3.4. Effect of compounds on tubulin polymerization

Next, four highly active compounds **4m**, **5d**, **5e**, and **5f** were evaluated for their ability to inhibit tubulin polymerization *in vitro* using the typical tubulin inhibitor CA-4 as the positive control. The assay presented in Table 3 suggested that these analogues notably blocked tubulin polymerization, and inhibition percentages were 49, 94, and 79 for compounds **5d**, **5e**, and CA-4, respectively, at the concentration of 10 μM. As shown in Fig. 7, additional screening indicated that **5e**, the greatest compound for antiproliferative activity, also displayed the best IC_{50} value (1.3 μM), in contrast to CA-4 (IC_{50} = 4.22 μM). The results revealed that effect on the tubulin polymerization positively correlated well with antiproliferative activity, indicating that these [1,2,4]triazolo[1,5-a]pyrimidines were potent tubulin polymerization inhibitors.

To verify whether analogues **5e** and colchicine occupy the same binding site in tubulin, a fluorescence based assay was carried out, according to our previously reported method [28]. And the results (Fig. 8) indicated that **5e** competitively inhibited colchicine binding to tubulin in a concentration-dependent manner. Therefore, that **5e** binds at the colchicine binding site of tubulin.

3.5. Molecular studies

To gain the potential binding features for the greatest derivative **5e** in the tubulin, a series of molecular docking simulations were carried out using the co-crystallized structure of tubulin with CA-4 (PDB: 5lyj). Overview of the binding site possessing the best

Table 2
Growth inhibitory effects of several compounds toward A549, HCT-116, HepG2, and the normal human embryonic kidney cell line HEK293.

comp.	IC_{50} mean ± SD[a] (μM)					
	T47D	HT29	A549	HCT-116	HepG2	HEK293
4m	>100	11.47 ± 1.64	>100	91.06 ± 4.33	41.19 ± 0.66	>100
5d	6.51 ± 0.54	83.05 ± 7.01	18.91 ± 1.16	>100	21.06 ± 0.52	>100
5e	3.49 ± 0.97	0.24 ± 0.07	6.05 ± 4.67	18.43 ± 1.34	14.69 ± 0.51	>100
5f	5.67 ± 0.29	1.66 ± 0.35	34.65 ± 1.14	22.44 ± 0.62	>100	82.14 ± 1.69
CA-4	0.027 ± 0.01	1.96 ± 0.61	0.021 ± 0.005	6.10 ± 0.14	5.29 ± 0.05	45.69 ± 5.15

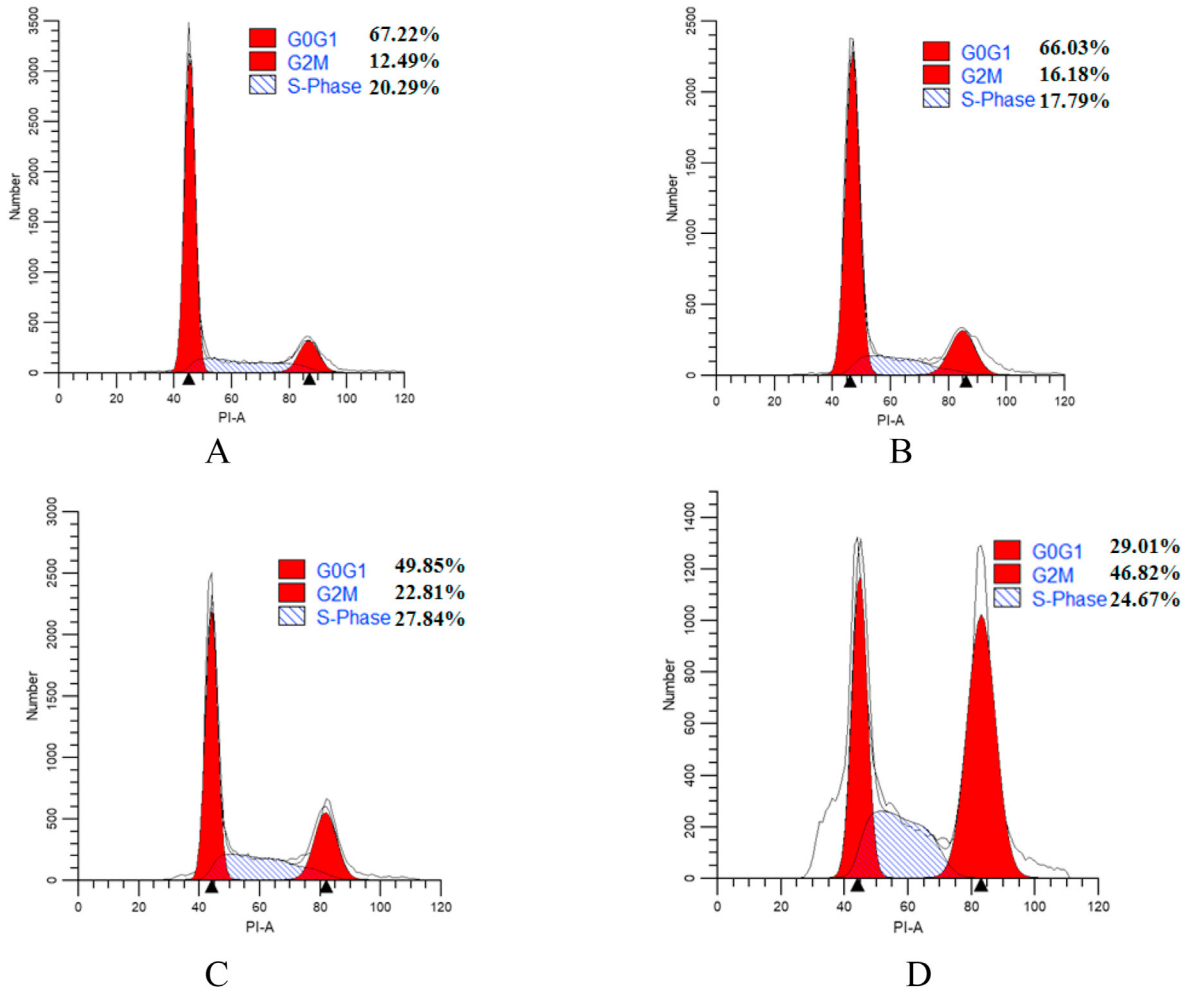

Fig. 3. Effects of **5e** on HeLa cell cycle progress. Flow cytometry analysis of HeLa stained by propidium iodide and treated using **5e** for 24 h. (A) Control; (B) **5e**, 30 nM; (C) **5e**, 60 nM; (D) **5e**, 120 nM.

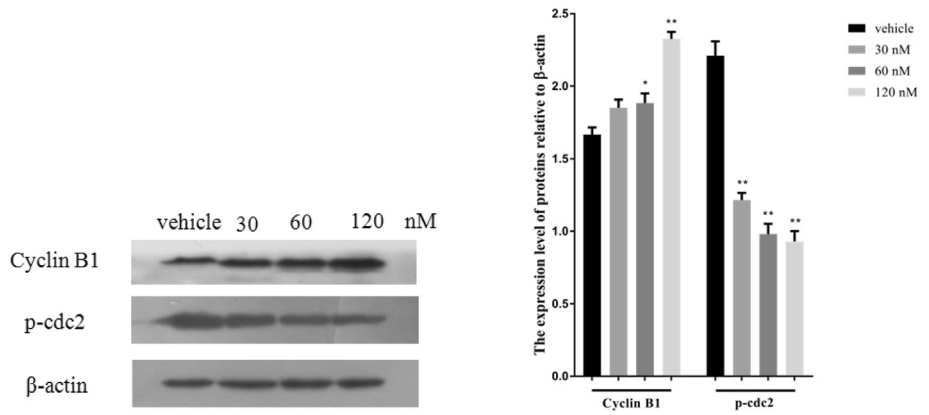

Fig. 4. Effects of **5e** on some G2/M regulatory proteins. HeLa cells were harvested and lysed for the detection of cyclin B1 and p-cdc2 expressions by western blot analysis. Data are presented as the mean ± SD of three independent experiments. *P < 0.05, **P < 0.01 vs the control.

docking score was shown in Fig. 9. Of interest is that **5e** adopts pretty similar location with CA-4 in the colchicine-binding site which is located on the interface between α/β-subunits and extended slightly out toward β-subunit. The triazolopyrimidine ring of the **5e** went deep into the pocket, and the nitrogen atom at *N*-4 position provided two potential hydrogen bond interactions with the Asn258 of α chain. Furthermore, the 3- hydroxyl group of 3-hydroxyl-4-methyloxyphenyl ring established a hydrogen bond with α-Val181. Notably, a critical hydrogen bond was observed between one of the oxygen atoms in 3,4,5-trimethoxylphenyl group and thiol hydrogen of β-Cys241 which is a typical interaction frequently reported for tubulin polymerization inhibitors

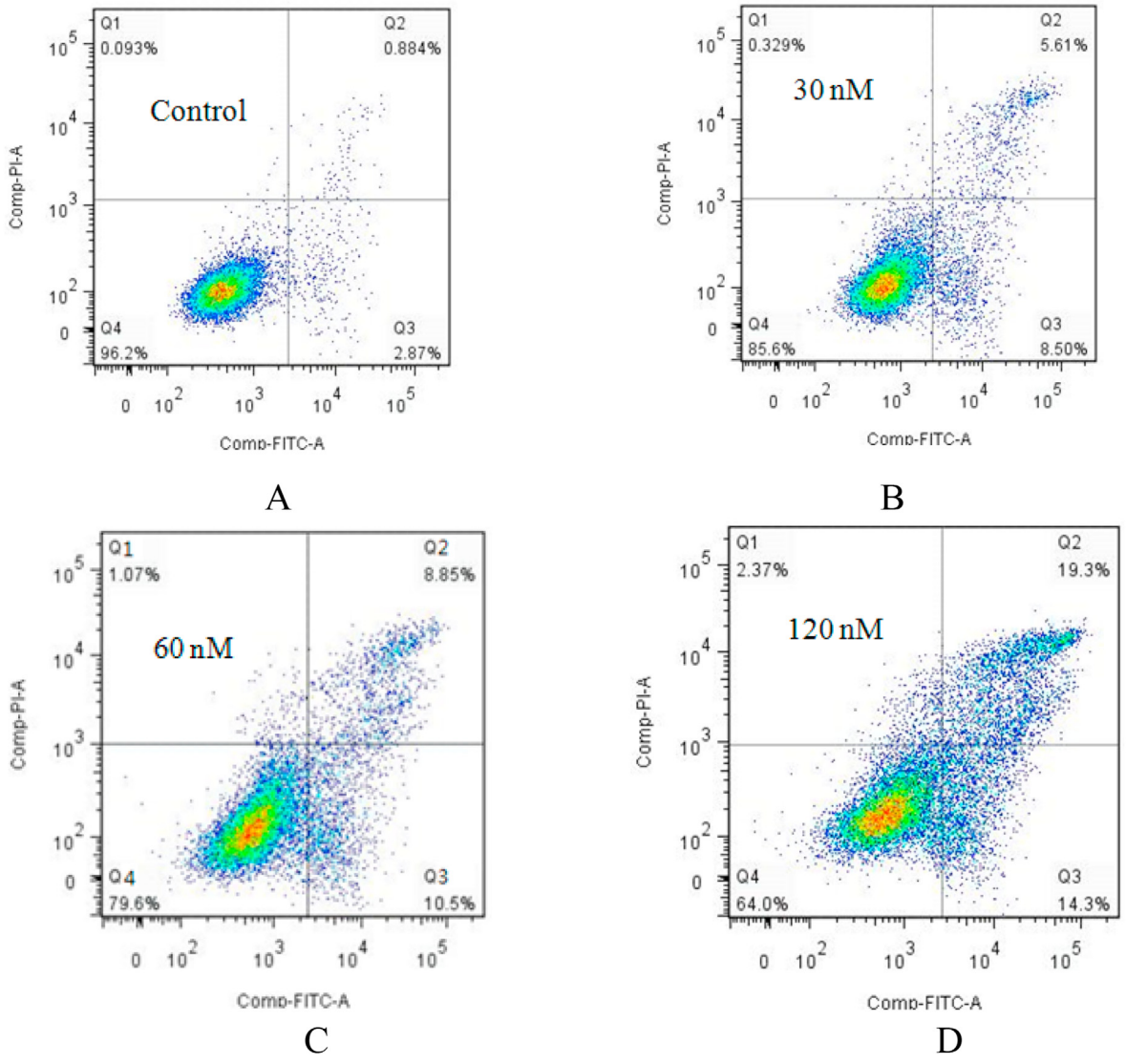

Fig. 5. Analyses of apoptosis induction in Hela cells. Detection of apoptotic cells after Annexin-V/PI staining by flow cytometry analysis. Cells were harvested and stained with Annexin-V/PI for analysis after treatment with different concentrations of compound **5e** (30, 60 and 120 nM) and control (untreated cells) for 24 h. The diverse cell stages were given as live (Q4), early apoptotic (Q3), late apoptotic (Q2), and necrotic cells (Q1).

binding in colchicine-site [37,38]. All these observations indicated that **5e** was a novel potential tubulin inhibitor targeting at the colchicine-binding site.

4. Conclusion

We have synthesized a series of new 2,7-diaryl- [1,2,4]triazolo [1,5-*a*]pyrimidines as potential tubulin polymerization inhibitors, through removing 5-methyl and 6-acetyl groups in our previously reported compound **3**. Some analogus exhibited increased anti-proliferative activities in the nanomolar range toward HeLa cells, and the most potent analogue **5e** possessed 166-fold improvement than the parent compound **3** for antiproliferative efficacies in HeLa cells. Interestingly, **5e** demonstrated significant selectivity in inhibiting cancer cells over HEK-293, a normal human embryonic kidney cell line. Further mechanism analysis suggested that **5e** dose-dependently caused G2/M arrest in HeLa cells through the alterations in the expression of p-cdc2 and cyclin B1, and induced cells apoptosis by up-regulating cleaved PARP expressions. Further evidence demonstrated that **5e** effectively inhibited tubulin polymerization and was 3-fold more potent than CA-4 (4.22 μM) with the IC_{50} value of 1.3 μM. The observations revealed that 2,7-diaryl- [1,2,4]triazolo[1,5-a]pyrimidine core might be used as the leading unit to develop novel tubulin polymerization inhibitors as potential anticancer agents.

5. Experimental section

5.1. General chemistry

^{1}H and ^{13}C NMR spectra were measured by a Mercury-Plus 400 spectrometer using DMSO-d_6 or $CDCl_3$ as solvents. Chemical shift (δ) is reported in ppm with tetramethylsilane (TMS) as internal reference. HRMS analyses were carried out through an Agilent QTOF 6540 mass spectrometer. Flash column chromatography was performed with silica gel (mesh 200−300), and reactions were monitored by TLC on 0.25 mm silicagel GF_{254} plates. Melting points (mp) were determined with a Buchi B-545 apparatus. Yields were of purified product and were not optimized. All starting materials were commercially available unless otherwise indicated.

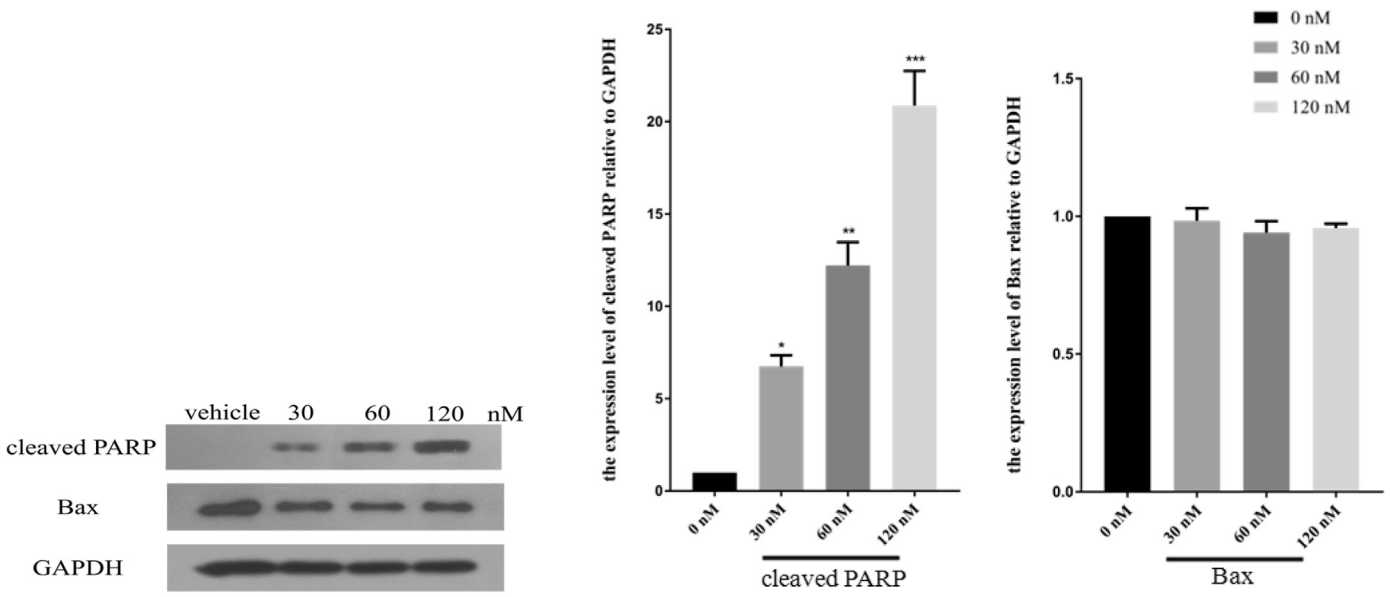

Fig. 6. Effects of **5e** on some apoptosis-related protein expression (cleaved PARP and Bax). Data are presented as the mean ± SD of three independent experiments. *P < 0.05, **P < 0.01 vs the control.

Table 3
Inhibitory activities of tubulin polymerization by four target compounds.

Comp.	R	Tubulin polymerization	
		%inhibition[a]	IC_{50}(μM)[b]
4m	3-NH_2-4-CH_3OPh	12	ND[c]
5d	3-NH_2-4-CH_3OPh	49	12.2 ± 0.6
5e	3-OH-4-CH_3OPh	94	1.3 ± 0.1
5f	3-CH_3CONH-4-CH_3OPh	16	ND
CA-4/		79	4.22 ± 0.15

[a] Samples were determined at 10 μM concentration.
[b] IC_{50} values were shown as the mean ± SD of three independent experiments.
[c] ND: Not determined.

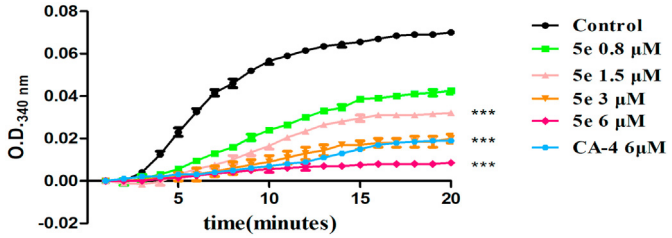

Fig. 7. Effect of compound **5e** on tubulin polymerization. Purified tubulin protein at 2 mg/mL in a reaction buffer incubated at 37 °C in the presence of **5e** (0.8, 1.5, 3, 6 μM), CA-4 (6 μM) or vehicle DMSO. Tubulin polymerization reaction was monitored at OD340 nm every minute at 37 °C over a 20 min period. Data were expressed as the mean ± SD from at least three independent experiments. ***P < 0.001 vs the control.

5.2. *Procedure for synthesis of intermediates **9**, **16a**–**u**, and **12a**–**u***

The intermediates 3-substituted 5-amino-1,2,4-triazoles **9** and **16a**–**u** were prepared according to reported procedures [34]. Arylpropenones **12a**–**u** were synthesized through the following procedure: A solution of 1-arylethanones **10** or **17** (2 mmol) and DMF-DMA (8 mL) was stirred at 90 °C for 4–6 h, then was poured into water, extracted with EtOAc, and dried. The EtOAc was then distilled off and the product was washed with cold petroleum ether to afford the compounds **12a**–**u**, respectively.

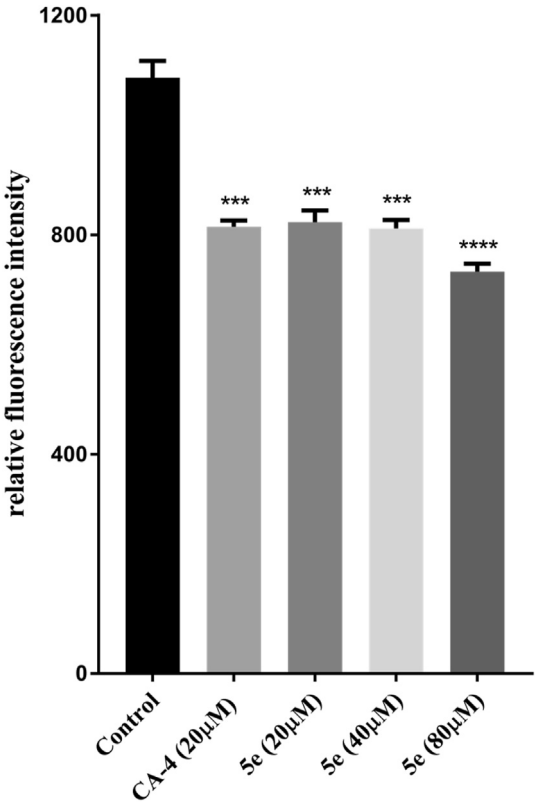

Fig. 8. Plot of fluorescence intensity of formation of the tubulin-colchicine complex by various concentrations of compound **5e**. Tubulin-compound **5e** complex was formed by incubating 4 μM tubulin with compound **5e** (20, 40, 80 μM) and CA-4 (20 μM) for 45 min at 37 °C. 4 μM colchicine was then added to the solution of this complex to get tubulin-colchicine complex. Fluorescence spectra were recorded (excitation at 340 nm, emission at 435 nm) after incubating for 45 min at 37 °C by using a Tecan Spark multimode reader. Spectra comprised of multiple scans from which blank values (buffer alone) were subtracted. ***P < 0.001, ****P < 0.0001 vs the control.

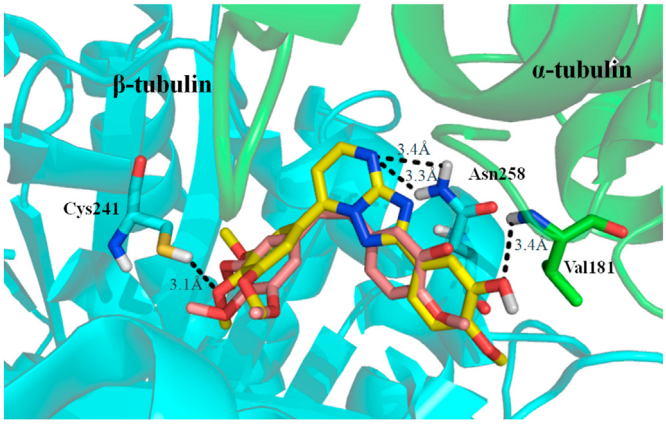

Fig. 9. Docking of **5e** (amber stick) into the colchicine-site of tubulin (PDB code: 5lyj), and overlapping with CA-4 (yellow stick).

*5.2.1. 3-(3,4,5-trimethoxyphenyl)-1H-1,2,4-triazol-5-amine (**9**)*

Yield, 71%; mp: 189.1–191.9 °C; ^{1}H NMR (400 MHz, DMSO-d_6) δ: 3.69 (s, 3H, CH_3O), 3.82 (s, 6H, 2 × CH_3O), 6.03 (s, 2H, NH_2), 7.19 (s,2H, ArH), 12.04 (s, 1H, NH).

*5.2.2. 3-(3,4-dichlorophenyl)-1H-1,2,4-triazol-5-amine (**16a**)*

Yield, 60%; mp: >300 °C; ^{1}H NMR (400 MHz, DMSO-d_6) δ: 6.17 (s, 2H, NH_2), 7.67 (d, J = 8.4 Hz, 1H, ArH), 7.83 (dd, J_1 = 1.6 Hz, J_2 = 8.4 Hz 1H, ArH), 8.00 (d, J = 1.6 Hz, 1H, ArH), 12.43 (s, 1H, NH).

*5.2.3. 3-(4-methoxyphenyl)-1H-1,2,4-triazol-5-amine (**16b**)*

Yield, 69%; mp: 223.1–225.0 °C; ^{1}H NMR (400 MHz, DMSO-d_6) δ: 3.79 (s, 3H, CH_3O), 6.19 (s, 2H, NH_2), 6.98 (d, J = 8.8 Hz, 2H, ArH), 7.82 (d, J = 8.8 Hz, 2H, ArH), 12.42 (s, 1H, NH).

*5.2.4. 3-(p-tolyl)-1H-1,2,4-triazol-5-amine (**16c**)*

Yield, 58%; mp: 209.5–211.2 °C; ^{1}H NMR (400 MHz, DMSO-d_6) δ: 2.37 (s, 3H, CH_3), 6.17 (s, 2H, NH_2), 7.34 (d, J = 8.0 Hz, 2H, ArH), 7.69 (d, J = 8.4 Hz, 2H, ArH), 12.21 (s, 1H, NH).

*5.2.5. 3-(3-amino-4-methoxyphenyl)-1H-1,2,4-triazol-5-amine (**16d**)*

Yield, 75%; mp: 184.3–185.9 °C; ^{1}H NMR (400 MHz, DMSO-d_6) δ: 3.82 (s, 3H, CH_3O), 4.98 (s, 2H, NH_2), 6.11 (s, 2H, NH_2), 6.94 (d, J = 8.4 Hz, 1H, ArH), 7.28 (d, J = 1.6 Hz, 1H, ArH), 7.44 (d, J = 8.4 Hz, 1H, ArH), 12.14 (s, 1H, NH).

*5.2.6. 5-(5-amino-1H-1,2,4-triazol-3-yl)-2-methoxyphenol (**16e**)*

Yield, 67%; mp: 193.1–194.5 °C; ^{1}H NMR (400 MHz, DMSO-d_6) δ: 3.83 (s, 3H, CH_3O), 6.15 (s, 2H, NH_2), 6.98 (d, J = 8.4 Hz, 1H, ArH), 7.30 (s, 1H, ArH), 7.54 (d, J = 8.4 Hz, 1H, ArH), 9.21 (s, 1H, OH), 12.31 (s, 1H, NH).

*5.2.7. N-(5-(5-amino-1H-1,2,4-triazol-3-yl)-2-methoxyphenyl) acetamide (**16f**)*

Yield, 62%; mp: 194.3–195.5 °C; ^{1}H NMR (400 MHz, DMSO-d_6) δ: 2.13 (s, 3H, CH_3), 3.82 (s, 3H, CH_3O), 6.13 (s, 2H, NH_2), 7.19 (d, J = 8.4 Hz, 1H, ArH), 7.67 (s, 1H, ArH), 7.88 (d, J = 8.4 Hz, 1H, ArH), 9.12 (s, 1H, NH), 12.22 (s, 1H, NH).

*5.2.8. (E)-1-(3,4-dimethoxyphenyl)-3-(dimethylamino)prop-2-en-1-one (**12a**)*

Yield, 78%; mp: 112.1–113.8 °C; ^{1}H NMR (400 MHz, $CDCl_3$) δ: 2.91 (s, 3H, CH_3), 3.09 (s, 3H, CH_3), 3.83 (s, 3H, CH_3O), 3.90 (s, 3H, CH_3O),5.73 (d, J = 12.0 Hz, 1H, CH), 7.01 (d, J = 8.4 Hz, 1H, ArH), 7.65 (dd, J_1 = 2.0 Hz, J_2 = 8.4 Hz,1H, ArH), 7.79 (d, J = 12.0 Hz, 1H, CH), 7.90 (d, J = 2.0 Hz,1H, ArH).

*5.2.9. (E)-3-(dimethylamino)-1-(p-tolyl)prop-2-en-1-one (**12b**)*

Yield, 72%; mp: 89.0–90.9 °C, Lit. 94–96 °C [35]; ^{1}H NMR (400 MHz, $CDCl_3$) δ: 2.49 (s, 3H, CH_3), 2.89 (s, 3H, CH_3), 3.07 (s, 3H, CH_3), 5.71 (d, J = 12.0 Hz, 1H, CH), 7.22 (d, J = 8.0 Hz, 2H, ArH),7.81 (d, J = 12.0 Hz, 1H, CH),8.01 (d, J = 8.0 Hz, 2H, ArH).

*5.2.10. (E)-3-(dimethylamino)-1-(3,4,5-trimethoxyphenyl)prop-2-en-1-one (**12c**)*

Yield, 53%; mp: 125.1–127.0 °C, Lit. 123–125 °C [36]; ^{1}H NMR (400 MHz, DMSO-d_6) δ: 2.94 (s, 3H, CH_3), 3.15 (s, 3H, CH_3), 3.71 (s, 3H, CH_3O), 3.85 (s, 6H, 2 × CH_3O), 5.83 (d, J = 12.4 Hz, 1H, CH), 7.18 (s, 2H, ArH), 7.70 (d, J = 12.0 Hz, 1H, CH).

*5.2.11. (E)-3-(dimethylamino)-1-(4-(trifluoromethyl)phenyl)prop-2-en-1-one (**12d**)*

Yield, 65%; mp: 88.1–89.9 °C, Lit. 88–90 °C [34]; ^{1}H NMR (400 MHz, $CDCl_3$) δ: 2.90 (s, 3H, CH_3), 3.12 (s, 3H, CH_3), 5.71 (d, J = 12.0 Hz, 1H, CH), 7.70 (d, J = 8.0 Hz, 2H, ArH), 7.78 (d, J = 12.0 Hz, 1H, CH),7.98 (d, J = 8.0 Hz, 2H, ArH).

*5.2.12. (E)-3-(dimethylamino)-1-(3-fluoro-4-methoxyphenyl)prop-2-en-1-one (**12e**)*

Yield, 74%; mp: 100.2–102.1 °C; ^{1}H NMR (400 MHz, $CDCl_3$) δ: 2.91 (s, 3H, CH_3), 3.12 (s, 3H, CH_3), 3.92 (s, 3H, CH_3O), 5.75 (d, J = 12.0 Hz, 1H, CH), 7.03 (d, J = 8.8 Hz, 1H, ArH), 7.76 (d, J = 12.0 Hz, 1H, CH), 7.89 (d,J = 8.4 Hz, 1H, ArH), 8.01 (d, J = 12.0 Hz, 1H, ArH).

*5.2.13. (E)-3-(dimethylamino)-1-(o-tolyl)prop-2-en-1-one (**12f**)*

Yield, 78%; mp: 95.1–97.0 °C; ^{1}H NMR (400 MHz, $CDCl_3$) δ: 2.26 (s, 3H, CH_3), 2.92 (s, 3H, CH_3), 3.12 (s, 3H, CH_3), 5.78 (d, J = 12.0 Hz, 1H, CH), 7.24 (t, J = 8.0 Hz, 2H, ArH), 7.32 (d, J = 7.6 Hz, 1H, ArH), 7.39 (d, J = 7.2 Hz, 1H, ArH), 7.73 (d, J = 12.0 Hz, 1H, CH).

*5.2.14. (E)-N-(4-(3-(dimethylamino)acryloyl)phenyl)acetamide (**12g**)*

Yield, 56%; mp: 151.9–153.2 °C; ^{1}H NMR (400 MHz, $CDCl_3$) δ: 2.17 (s, 3H, CH_3), 2.93 (s, 3H, CH_3), 3.08 (s, 3H, CH_3), 5.71 (d, J = 12.0 Hz, 1H, CH), 7.62 (d, J = 7.6 Hz, 2H, ArH), 7.76 (d, J = 12.0 Hz, 1H, CH), 7.85 (d, J = 8.0 Hz, 2H, ArH), 8.74 (s, 1H, NH).

*5.2.15. (E)-methyl 4-(3-(dimethylamino)acryloyl)benzoate (**12h**)*

Yield, 62%; mp: 110.5–111.9 °C; ^{1}H NMR (400 MHz, $CDCl_3$) δ: 2.97 (s, 3H, CH_3), 3.19 (s, 3H, CH_3), 3.95 (s, 3H, CH_3O), 5.72 (d, J = 12.4 Hz, 1H, CH), 7.84 (d, J = 12.4 Hz, 1H, CH), 7.94 (d, J = 7.6 Hz, 2H, ArH), 8.09 (d, J = 7.6 Hz, 2H, ArH).

*5.2.16. (E)-3-(dimethylamino)-1-(4-methoxy-3-nitrophenyl)prop-2-en-1-one (**12i**)*

Yield, 76%; mp: 163.1–165.0 °C; ^{1}H NMR (400 MHz, $CDCl_3$) δ: 2.98 (s, 3H, CH_3), 3.19 (s, 3H, CH_3), 4.02 (s, 3H, CH_3O), 5.67 (d, J = 12.0 Hz, 1H, CH), 7.13 (d, J = 8.4 Hz, 1H, ArH), 7.86 (d, J = 12.0 Hz, 1H, CH), 8.19 (d, J = 8.8 Hz, 1H, ArH), 8.40 (s, 1H, ArH).

*5.2.17. (E)-3-(dimethylamino)-1-(4-methoxyphenyl)prop-2-en-1-one (**12j**)*

Yield, 81%; mp: 109.4–111.3 °C, Lit. 113–115 °C [36]; ^{1}H NMR (400 MHz, $CDCl_3$) δ: 2.91 (s, 3H, CH_3), 3.13 (s, 3H, CH_3), 3.81 (s, 3H, CH_3O), 5.81 (d, J = 12.0 Hz, 1H, CH), 6.97 (d, J = 8.4 Hz, 2H, ArH), 7.67 (d, J = 12.4 Hz, 1H, CH), 7.89 (d, J = 8.4 Hz, 2H, ArH).

*5.2.18. (E)-1-(3,4-dichlorophenyl)-3-(dimethylamino)prop-2-en-1-one (**12k**)*

Yield, 73%; mp: 94.1–95.7 °C; ^{1}H NMR (400 MHz, $CDCl_3$) δ: 2.95 (s, 3H, CH_3), 3.17 (s, 3H, CH_3), 5.91 (d, J = 12.0 Hz, 1H, CH), 7.76 (d, J = 8.8 Hz, 1H, ArH), 7.93 (d, J = 12.0 Hz, 1H, CH), 8.21 (dd, J_1 = 2.0 Hz, J_2 = 8.4 Hz, 1H, ArH), 8.33 (d, J = 2.0 Hz, 1H, ArH).

*5.2.19. (E)-1-(3-chloro-4-methoxyphenyl)-3-(dimethylamino)prop-2-en-1-one (**12l**)*

Yield, 77%; mp: 124.6–126.1 °C; ^{1}H NMR (400 MHz, $CDCl_3$) δ: 2.94 (s, 3H, CH_3), 3.13 (s, 3H, CH_3), 3.74 (s, 3H, CH_3O), 5.81 (d, J = 12.0 Hz, 1H, CH), 7.23 (d, J = 8.8 Hz, 1H, ArH),7.80 (d, J = 12.0 Hz, 1H, CH), 8.18 (dd, J_1 = 2.0 Hz, J_2 = 8.8 Hz, 1H, ArH), 8.39 (d, J = 2.0 Hz, 1H, ArH).

*5.2.20. (E)-N-(2,6-dichloro-4-(3-(dimethylamino)acryloyl)phenyl) acetamide (**12n**)*

Yield, 62%; mp: 196.5–197.9 °C; ^{1}H NMR (400 MHz, $CDCl_3$) δ: 2.13 (s, 3H, CH_3), 2.99 (s, 3H, CH_3), 3.15 (s, 3H, CH_3), 5.90 (d, J = 12.0 Hz, 1H, CH), 7.97 (d, J = 12.0 Hz, 1H, CH), 8.25 (s,2H, ArH), 10.05 (s, 1H, NH).

*5.2.21. (E)-3-(dimethylamino)-1-(4-nitrophenyl)prop-2-en-1-one (**12o**)*

Yield, 59%; mp: 151.2–153.5 °C; ^{1}H NMR (400 MHz, $CDCl_3$) δ: 2.95 (s, 3H, CH_3), 3.13 (s, 3H, CH_3), 5.94 (d, J = 12.0 Hz, 1H, CH), 7.90 (d, J = 12.0 Hz, 1H, CH), 8.20 (d, J = 8.8 Hz, 2H, ArH), 8.46 (d, J = 8.4 Hz, 2H, ArH).

*5.2.22. (E)-3-(dimethylamino)-1-(furan-2-yl)prop-2-en-1-one (**12q**)*

Yield, 76%; mp: 92.6–93.7 °C; ^{1}H NMR (400 MHz, $CDCl_3$) δ: 2.92 (s, 3H, CH_3), 3.07 (s, 3H, CH_3), 5.62 (d, J = 12.0 Hz, 1H, CH), 6.78 (d, J = 3.6 Hz, 1H, ArH), 7.53 (d, J = 12.0 Hz, 1H, CH), 7.68 (s, 1H, ArH), 8.29 (d, J = 3.2 Hz, 1H, ArH).

*5.2.23. (E)-3-(dimethylamino)-1-(naphthalen-1-yl)prop-2-en-1-one (**12r**)*

Yield, 82%; mp: 91.1–93.0 °C; ^{1}H NMR (400 MHz, $CDCl_3$) δ: 2.91 (s, 3H, CH_3), 3.09 (s, 3H, CH_3), 5.71 (d, J = 12.0 Hz, 1H, CH),7.54 (d, J = 8.8 Hz, 2H, ArH), 7.58 (d, J = 6.8 Hz,1H, ArH), 7.67 (t, J = 7.6 Hz, 1H, ArH), 7.72 (d, J = 12.0 Hz, 1H, CH), 7.81 (d, J = 6.4 Hz, 1H, ArH),7.89 (d, J = 8.0 Hz, 1H, ArH), 8.14 (d, J = 8.4 Hz, 1H, ArH).

*5.2.24. (E)-3-(dimethylamino)-1-(thiophen-2-yl)prop-2-en-1-one (**12s**)*

Yield, 74%; mp: 107.5–109.4 °C, Lit. 106–108 °C [35]; ^{1}H NMR (400 MHz, $CDCl_3$) δ: 2.90 (s, 3H, CH_3), 3.11 (s, 3H, CH_3), 5.72 (d, J = 12.0 Hz, 1H, CH), 7.21 (t, J = 4.4 Hz, 1H, ArH), 7.69 (d, J = 12.0 Hz, 1H, CH), 7.81 (d, J = 5.2 Hz, 1H, ArH), 8.16 (d, J = 3.6 Hz, 1H, ArH).

*5.2.25. (E)-3-(dimethylamino)-1-(pyridin-3-yl)prop-2-en-1-one (**12t**)*

Yield, 81%; mp: 79.8–81.4 °C, Lit. 72–74 °C [35]; ^{1}H NMR (400 MHz, $CDCl_3$) δ: 2.95 (s, 3H, CH_3), 3.13 (s, 3H, CH_3), 5.75 (d, J = 12.0 Hz, 1H, CH), 7.21 (d, J = 3.6 Hz, 1H, ArH), 7.73 (d, J = 12.0 Hz, 1H, CH), 8.31 (d, J = 7.6 Hz, 1H, ArH), 8.67 (s, 1H, ArH), 9.12 (s, 1H, ArH).

*5.2.26. (E)-3-(3-(dimethylamino)acryloyl)-2H-chromen-2-one (**12u**)*

Yield, 76%; mp: 161.1–163.2 °C; ^{1}H NMR (400 MHz, $CDCl_3$) δ: 2.91 (s, 3H, CH_3), 3.12 (s, 3H, CH_3), 5.78 (d, J = 12.0 Hz, 1H, CH), 7.40 (t, J = 8.0 Hz, 2H, ArH), 7.67 (d, J = 12.0 Hz, 1H, CH), 7.72 (d, J = 8.0 Hz, 2H, ArH), 9.21 (s, 1H, ArH).

*5.3. Procedure for synthesis of compounds **4a–u** and **5a–f***

To a solution of 3-substituted 5-amino-1,2,4-triazoles **9** or **16** (1 mmol) in 6 mL of glacial acetic acid (or 8 mL of ethanol with catalytic amount of HCl for preparation of 4 m, 4p, 5d, 5e) was added to appropriate 3-(dimethylamino)prop-2-en-1-one **12** (1 mmol), and the resulting mixtures were stirred for 2–5 h at 80 °C, and detected by TLC. After cooling, the reaction mixtures were poured into ice/water, extracted with EtOAc, washed with H_2O, then dried in vacuum to provide a precipitate, which was crystallized by ethanol to afford the desired compounds **4a–u** and **5a–f**.

*5.3.1. 7-(3,4-Dimethoxy-phenyl)-2-(3,4,5-trimethoxy-phenyl)-[1,2,4]triazolo[1,5-a]pyrimidine (**4a**)*

Yield, 68%; mp: 228.9–229.8 °C; ^{1}H NMR (400 MHz, $CDCl_3$) δ: 3.95 (s, 3H, CH_3O), 3.99 (s, 6H, 2 × CH_3O), 4.04 (s, 3H, CH_3O),4.06 (s, 3H, CH_3O), 7.11 (d, J = 8.4 Hz, 1H, ArH), 7.22 (d, J = 4.8 Hz, 2H, ArH), 7.67 (s, 2H, ArH), 7.80 (dd, J_1 = 2.0 Hz, J_2 = 8.4 Hz,1H, ArH), 8.12 (d, J = 2.0 Hz, 1H, ArH), 8.79 (d, J = 4.8 Hz, 1H, ArH). ^{13}C NMR (100 MHz, $CDCl_3$) δ: 165.22, 153.72, 153.37, 152.06, 148.71, 147.18, 140.11, 125.81, 123.08, 122.07, 112.52, 111.05, 107.77, 104.48, 60.92, 56.15, 56.09, 55.96. HRMS (ESI) *m/z*: calcd for $C_{22}H_{22}N_4O_5$ (M + H^+) 423.1663 found 423.1667.

*5.3.2. 7-p-Tolyl-2-(3,4,5-trimethoxy-phenyl)-[1,2,4]triazolo[1,5-a] pyrimidine (**4b**)*

Yield, 65%; mp: 187.0–187.4 °C; ^{1}H NMR (400 MHz, $CDCl_3$) δ: 2.53 (s, 3H, CH_3), 3.94 (s, 3H, CH_3O), 4.00 (s, 6H, 2 × CH_3O), 7.19 (d, J = 4.4 Hz, 1H, ArH), 7.46 (d, J = 8.0 Hz, 2H, ArH), 7.66 (s, 2H, ArH), 8.15 (d, J = 8.0 Hz, 2H, ArH), 8.80 (d, J = 4.4 Hz, 1H, ArH). ^{13}C NMR (100 MHz, $CDCl_3$) δ: 165.45, 157.23, 153.82, 153.39, 147.75, 142.56, 140.24, 129.58, 129.34, 126.97, 125.86, 108.40, 104.82, 60.90, 56.30, 21.60. HRMS (ESI) *m/z*: calcd for $C_{21}H_{20}N_4O_3$(M + H^+) 377.1608 found 377.1609.

*5.3.3. 2,7-Bis-(3,4,5-trimethoxy-phenyl)-[1,2,4]triazolo[1,5-a] pyrimidine (**4c**)*

Yield, 59%; mp: 268.1–268.9 °C; ^{1}H NMR (400 MHz, $CDCl_3$) δ: 3.95 (s, 3H, CH_3O), 3.99 (s, 6H, 2 × CH_3O), 4.02 (s, 9H, 3 × CH_3O), 7.24 (d, J = 4.4 Hz, 1H, ArH), 7.60 (s, 2H, ArH), 7.67 (s, 2H, ArH), 8.82 (d, J = 4.0 Hz, 1H, ArH). ^{13}C NMR (100 MHz, $CDCl_3$) δ: 165.40, 157.35, 153.80, 153.41, 153.28, 147.14, 141.34, 140.25, 125.69, 124.56, 108.19, 107.15, 104.52, 61.05, 60.92, 56.31, 56.15. HRMS (ESI) *m/z*: calcd for $C_{23}H_{24}N_4O_6$ (M + H^+) 453.1769 found 453.1768.

*5.3.4. 7-(4-Trifluoromethyl-phenyl)-2-(3,4,5-trimethoxy-phenyl)-[1,2,4]triazolo[1,5-a]pyrimidine (**4d**)*

Yield, 61%; mp: 198.1–198.7 °C; ^{1}H NMR (400 MHz, $CDCl_3$) δ: 3.94 (s, 3H, CH_3O), 3.99 (s, 6H, 2 × CH_3O), 7.23 (d, J = 4.0 Hz, 1H, ArH), 7.63 (s, 2H, ArH), 7.92 (d, J = 8.0 Hz, 2H, ArH), 8.34 (d, J = 8.0 Hz, 2H, ArH), 8.88 (d, J = 4.0 Hz, 1H, ArH).^{13}C NMR (100 MHz, $CDCl_3$) δ: 165.88, 157.06, 153.99, 153.45, 145.98, 140.47, 133.25, 129.81, 125.86, 125.83, 125.43, 122.15, 109.13, 104.83, 60.91, 56.31. HRMS (ESI) *m/z*: calcd for $C_{21}H_{17}F_3N_4O_3$ (M + H^+) 431.1326 found 431.1325.

*5.3.5. 7-(3-Fluoro-4-methoxy-phenyl)-2-(3,4,5-trimethoxy-phenyl)-[1,2,4]triazolo[1,5-a]pyrimidine (**4e**)*

Yield, 70%; mp: 174.6–175.6 °C; ^{1}H NMR (400 MHz, $CDCl_3$) δ: 3.95 (s, 3H, CH_3O), 4.00 (s, 6H, 2 × CH_3O), 4.04 (s, 3H, CH_3O), 7.18 (d, J = 4.0 Hz, 1H, ArH), 7.21 (d, J = 8.8 Hz, 1H, ArH), 7.65 (s, 2H, ArH), 8.05 (d, J = 8.4 Hz, 1H, ArH), 8.18 (d, J = 12.0 Hz, 1H, ArH),8.79 (d, J = 4.4 Hz, 1H, ArH).^{13}C NMR (100 MHz, $CDCl_3$) δ: 165.52, 157.24, 153.74, 153.42, 150.66, 146.02, 140.33, 126.28, 125.66, 122.18, 117.32,

113.17, 113.15, 107.92, 104.79, 60.91, 56.34, 56.29. HRMS (ESI) *m/z*: calcd for $C_{21}H_{19}FN_4O_4$ (M + H^+) 411.1463 found 411.1463.

*5.3.6. 7-o-Tolyl-2-(3,4,5-trimethoxy-phenyl)-[1,2,4]triazolo[1,5-a] pyrimidine (**4f**)*

Yield, 67%; mp: 160.9−161.5 °C; ^{1}H NMR (400 MHz, $CDCl_3$) δ: 2.27 (s, 3H, CH_3), 3.92 (s, 3H, CH_3O), 3.96 (s, 6H, 2 × CH_3O), 7.03 (s, 1H, ArH), 7.44 (t, *J* = 8.0 Hz, 2H, ArH), 7.50 (d, *J* = 7.6 Hz, 1H, ArH), 7.54 (d, *J* = 7.2 Hz, 1H, ArH), 7.59 (s, 2H, ArH), 8.83 (s, 1H, ArH).^{13}C NMR (100 MHz, $CDCl_3$) δ: 165.71, 156.61, 153.64, 153.36, 148.99, 140.24, 137.50, 130.87, 130.78, 130.17, 129.63, 126.07, 125.76, 110.83, 104.82, 60.88, 56.31, 20.06. HRMS (ESI) *m/z*: calcd for $C_{21}H_{20}N_4O_3$ (M + H^+) 377.1608 found 377.1610.

*5.3.7. N-(4-(2-(3,4,5-trimethoxyphenyl)-[1,2,4]triazolo[1,5-a] pyrimidin-7-yl)phenyl)acetamide (**4g**)*

Yield, 63%; mp: 236.8−237.2 °C; ^{1}H NMR (400 MHz, $CDCl_3$) δ: 2.28 (s, 3H, CH_3), 3.93 (s, 3H, CH_3O), 3.95 (s,6H,2 × CH_3O), 7.16 (d, *J* = 4.4 Hz, 1H, ArH), 7.59 (s, 2H, ArH), 7.86 (d, *J* = 8.0 Hz, 2H, ArH), 8.14 (s, 1H, NH), 8.24 (d, *J* = 8.4 Hz, 2H, ArH), 8.76 (d, *J* = 4.4 Hz, 1H, ArH). ^{13}C NMR (100 MHz, $CDCl_3$) δ: 168.90, 165.30, 157.16, 153.82, 153.35, 147.02, 141.41, 140.15, 130.49, 125.71, 124.90, 119.39, 108.18, 104.74, 60.89, 56.25, 24.66. HRMS (ESI) *m/z*: calcd for $C_{22}H_{21}N_5O_4$ (M + H^+) 420.1667 found 420.1666.

*5.3.8. 4-[2-(3,4,5-Trimethoxy-phenyl)-[1,2,4]triazolo[1,5-a] pyrimidin-7-yl]-benzoic acid methyl ester (**4h**)*

Yield, 71%; mp: 202.4−202.7 °C; ^{1}H NMR (400 MHz, $CDCl_3$) δ: 3.94 (s, 3H, CH_3O), 3.99 (s, 6H, 2 × CH_3O), 4.02 (s, 3H, CH_3O), 7.24 (s, 1H, ArH), 7.63 (s, 2H, ArH), 8.29 (s, 4H, ArH), 8.86 (s, 1H, ArH). ^{13}C NMR (100 MHz, $CDCl_3$) δ: 166.05, 165.75, 157.09, 153.94, 153.42, 146.44, 140.37, 133.84, 132.84, 129.91, 129.41, 125.51, 109.10, 104.76, 60.90, 56.28, 52.52. HRMS (ESI) *m/z*: calcd for $C_{22}H_{20}N_4O_5$ (M + H^+) 421.1507 found 421.1505.

*5.3.9. 7-(4-Methoxy-3-nitro-phenyl)-2-(3,4,5-trimethoxy-phenyl)-[1,2,4]triazolo[1,5-a]pyrimidine (**4i**)*

Yield, 73%; mp: 222.9−223.7 °C; ^{1}H NMR (400 MHz, DMSO-d_6) δ: 3.76 (s, 3H, CH_3O), 3.91 (s, 6H, 2 × CH_3O), 4.09 (s, 3H, CH_3O), 7.54 (s, 2H, ArH), 7.65 (d, *J* = 8.8 Hz, 1H, ArH), 7.77 (d, *J* = 4.0 Hz, 1H, ArH), 8.63 (d,*J* = 8.8 Hz, 1H, ArH), 8.91 (d,*J* = 3.6 Hz, 1H, ArH), 9.26 (s, 1H, ArH). ^{13}C NMR (100 MHz, DMSO-d_6) δ: 164.29, 157.08, 155.10, 154.87, 153.65, 144.47, 140.12, 139.07, 136.01, 127.61, 125.86, 121.66, 115.23, 109.28, 104.48, 60.59, 57.73, 56.29. HRMS (ESI) *m/z*: calcd for $C_{21}H_{19}N_5O_6$ (M + H^+) 438.1408 found 438.1408.

*5.3.10. 7-(4-Methoxy-phenyl)-2-(3,4,5-trimethoxy-phenyl)-[1,2,4] triazolo[1,5-a]pyrimidine (**4j**)*

Yield, 60%; mp: 174.2−174.6 °C; ^{1}H NMR (400 MHz, DMSO-d_6) δ: 3.76 (s, 3H, CH_3O), 3.91 (s, 9H, 3 × CH_3O), 7.23 (d,*J* = 8.8 Hz, 2H, ArH), 7.52 (s, 2H, ArH), 7.57 (d, *J* = 4.8 Hz, 1H, ArH), 8.37 (d, *J* = 8.8 Hz, 2H, ArH), 8.85 (d,*J* = 4.4 Hz, 1H, ArH). ^{13}C NMR (100 MHz, DMSO-d_6) δ: 164.35, 162.43, 157.17, 154.95, 153.65, 147.01, 140.13, 131.95, 126.16, 122.00, 114.69, 108.97, 104.72, 60.58, 56.44, 56.00. HRMS (ESI) *m/z*: calcd for $C_{21}H_{20}N_4O_4$ (M + H^+) 393.1558 found 393.1557.

*5.3.11. 7-(3,4-Dichloro-phenyl)-2-(3,4,5-trimethoxy-phenyl)-[1,2,4] triazolo[1,5-a]pyrimidine (**4k**)*

Yield, 63%; mp: 213.2−213.5 °C; ^{1}H NMR (400 MHz, DMSO-d_6) δ: 3.76 (s, 3H, CH_3O), 3.90 (s, 6H, 2 × CH_3O), 7.49 (s, 2H, ArH), 7.71 (d, *J* = 4.8 Hz, 1H, ArH), 7.96 (d, *J* = 8.8 Hz, 1H, ArH), 8.31 (dd, J_1 = 2.0 Hz, J_2 = 8.4 Hz, 1H, ArH), 8.61 (d, *J* = 2.0 Hz, 1H, ArH), 8.93 (d, *J* = 4.4 Hz, 1H, ArH). ^{13}C NMR (100 MHz, DMSO-d_6) δ: 165.77, 157.08, 153.91, 153.44, 144.97, 140.42, 136.34, 133.45, 131.35, 130.92, 129.43, 128.34, 125.35, 108.57, 104.73, 60.91, 56.24. HRMS (ESI) *m/z*: calcd for $C_{20}H_{16}C_{l2}N_4O_3$ (M + H^+) 431.0672 found 431.06720.

*5.3.12. 7-(3-Chloro-4-methoxy-phenyl)-2-(3,4,5-trimethoxy-phenyl)-[1,2,4]triazolo[1,5-a]pyrimidine (**4l**)*

Yield, 68%; mp: 206.3−206.7 °C; ^{1}H NMR (400 MHz, DMSO-d_6) δ: 3.76 (s, 3H, CH_3O), 3.90 (s, 6H, 2 × CH_3O), 4.01 (s, 3H, CH_3O), 7.43 (d, *J* = 8.8 Hz,1H, ArH), 7.50 (s, 2H, ArH), 7.65 (d, *J* = 4.8 Hz, 1H, ArH), 8.38 (dd, J_1 = 2.0 Hz, J_2 = 8.8 Hz, 1H, ArH), 8.55 (d, *J* = 2.0 Hz, 1H, ArH),8.85 (d, *J* = 4.8 Hz, 1H, ArH). ^{13}C NMR (100 MHz, DMSO-d_6) δ: 164.30, 157.50, 157.09, 154.96, 153.63, 145.47, 140.13, 131.52, 130.72, 126.01, 122.76, 121.68, 113.22, 109.19, 104.58, 60.57, 57.03, 56.34. HRMS (ESI) *m/z*: calcd for $C_{21}H_{19}ClN_4O_4$ (M + H^+) 427.1168 found 427.1163.

*5.3.13. 2-Methoxy-5-[2-(3,4,5-trimethoxy-phenyl)-[1,2,4]triazolo [1,5-a]pyrimidin-7-yl]- phenylamine (**4 m**)*

Yield, 79%; mp: 109.2−111.1 °C; ^{1}H NMR (400 MHz, DMSO-d_6) δ: 3.76 (s, 3H, CH_3O), 3.91 (s, 3H, CH_3O), 3.92 (s, 6H, 2 × CH_3O), 5.15 (s, 2H, NH_2), 7.07 (d, *J* = 8.4 Hz, 1H, ArH), 7.46 (d, *J* = 4.0 Hz, 1H, ArH), 7.56 (s, 2H, ArH), 7.60 (d, *J* = 8.4 Hz, 1H, ArH),7.75 (s, 1H, ArH),8.82 (d, *J* = 4.4 Hz, 1H, ArH). ^{13}C NMR (100 MHz, DMSO-d_6) δ: 164.31, 157.26, 154.84, 153.64, 149.65, 147.91, 140.05, 138.28, 126.24, 122.20, 119.06, 114.41, 110.75, 108.77, 104.76, 60.58, 56.43, 55.98. HRMS (ESI) *m/z*: calcd for $C_{21}H_{21}N_5O_4$ (M + H^+) 408.1667 found 408.1667.

*5.3.14. N-(2,6-dichloro-4-(2-(3,4,5-trimethoxyphenyl)-[1,2,4] triazolo[1,5-a]pyrimidin-7-yl)phenyl) acetamide (**4n**).* Yield, 52%; mp: 273.1−273.5 °C; ^{1}H NMR (400 MHz, DMSO-d_6) δ: 2.14 (s, 3H, CH_3), 3.76 (s, 3H, CH_3O), 3.89 (s, 6H, 2 × CH_3O), 7.49 (s, 2H, ArH), 7.76 (d, *J* = 4.8 Hz, 1H, ArH), 8.49 (s,2H, ArH), 8.95 (d, *J* = 4.4 Hz, 1H, ArH), 10.13 (s, 1H, NH). ^{13}C NMR (100 MHz, DMSO-d_6) δ: 168.72, 164.43, 156.91, 155.31, 153.65, 144.07, 140.17, 136.40, 134.07, 130.33, 129.87, 125.86, 110.51, 104.52, 60.59, 56.29, 22.88. HRMS (ESI) *m/z*: calcd for $C_{22}H_{19}Cl_2N_5O_4$ (M + H^+) 488.0887 found 488.0881.

*5.3.15. 7-(4-Nitro-phenyl)-2-(3,4,5-trimethoxy-phenyl)-[1,2,4] triazolo[1,5-a]pyrimidine(**4o**)*

Yield, 62%; mp: 246.8−247.2 °C; ^{1}H NMR (400 MHz, DMSO-d_6) δ: 3.76 (s, 3H, CH_3O), 3.90 (s, 6H, 2 × CH_3O), 7.51 (s, 2H, ArH), 7.72 (d, *J* = 4.4 Hz, 1H, ArH), 8.50 (d, *J* = 8.8 Hz, 2H, ArH), 8.56 (d, *J* = 8.4 Hz, 2H, ArH), 8.99 (d, *J* = 4.4 Hz, 1H, ArH). ^{13}C NMR (100 MHz, DMSO-d_6) δ: 164.61, 156.94, 155.46, 153.68, 149.34, 145.17, 140.27, 136.02, 131.57, 125.89, 124.13, 110.97, 104.78, 60.59, 56.48. HRMS (ESI) *m/z*: calcd for $C_{20}H_{17}N_5O_5$ (M + Na^+) 430.1122 found 430.1117.

*5.3.16. 4-(2-(3,4,5-trimethoxyphenyl)-[1,2,4]triazolo[1,5-a] pyrimidin-7-yl)aniline **(4p)***

Yield, 84%; mp: 239.1−240.1 °C; ^{1}H NMR (400 MHz, DMSO-d_6) δ: 3.76 (s, 3H, CH_3O), 3.92 (s, 6H, 2 × CH_3O), 6.14 (s, 2H, NH_2), 6.79 (d, *J* = 8.8 Hz, 2H, ArH), 7.47 (d, *J* = 5.2 Hz,1H, ArH), 7.54 (s, 2H, ArH), 8.25 (d, *J* = 8.8 Hz, 2H, ArH), 8.72 (d, *J* = 4.8 Hz, 1H, ArH). ^{13}C NMR (100 MHz, DMSO-d_6) δ: 164.07, 157.44, 154.32, 153.64, 153.14, 147.75, 140.01, 131.87, 126.36, 115.59, 113.60, 106.95, 104.65, 60.58, 56.39. HRMS (ESI) *m/z*: calcd for $C_{20}H_{19}N_5O_3$ (M + H^+) 378.1561 found 378.1563.

*5.3.17. 7-(furan-2-yl)-2-(3,4,5-trimethoxyphenyl)-[1,2,4]triazolo [1,5-a]pyrimidine (**4q**)*

Yield: 57%; mp: 206.8−207.7 °C; ^{1}H NMR (400 MHz, $CDCl_3$) δ: 3.97 (s,3H, CH_3O), 4.05 (s, 6H, 2 × CH_3O), 6.83 (dd, J_1 = 1.6 Hz, J_2 = 3.6 Hz, 1H, ArH), 7.54 (d, *J* = 4.8 Hz,1H, ArH), 7.72 (s, 2H, ArH), 7.82 (s, 1H, ArH), 8.33 (d, *J* = 3.2 Hz, 1H, ArH), 8.82 (d, *J* = 4.8 Hz, 1H, ArH).^{13}C NMR (100 MHz, $CDCl_3$) δ:165.67, 156.70, 153.43, 153.36,

146.61, 143.20, 140.32, 136.73, 125.76, 120.69, 113.46, 104.77, 104.03, 60.95, 56.30. HRMS (ESI) *m/z*: calcd for $C_{18}H_{16}N_4O_4$ (M + H^+) 353.1245 found 353.1244.

*5.3.18. 7-(naphthalen-1-yl)-2-(3,4,5-trimethoxyphenyl)-[1,2,4] triazolo[1,5-a]pyrimidine (**4r**)*

Yield, 69%; mp: 199.1–200.5 °C; ^{1}H NMR (400 MHz, $CDCl_3$) δ: 3.90 (s, 9H, 3 × CH_3O), 7.22 (d, *J* = 4.4 Hz, 1H, ArH), 7.50 (s, 2H, ArH), 7.58 (d, *J* = 8.8 Hz, 2H, ArH), 7.62 (d, *J* = 6.8 Hz,1H, ArH), 7.71 (t, *J* = 7.6 Hz, 1H, ArH), 7.87 (d, *J* = 6.4 Hz, 1H, ArH), 8.03 (d, *J* = 8.0 Hz, 1H, ArH), 8.16 (d, *J* = 8.4 Hz, 1H, ArH), 8.91 (d, *J* = 4.4 Hz, 1H, ArH). ^{13}C NMR (100 MHz, $CDCl_3$) δ: 165.65, 156.92, 153.67, 153.29, 147.66, 140.13, 133.63, 131.67, 130.40, 128.74, 128.54, 127.71, 127.24, 126.66, 125.69, 125.07, 124.86, 111.72, 104.78, 60.86, 56.23. HRMS (ESI) *m/z*: calcd for $C_{24}H_{20}N_4O_3$ (M + H^+) 413.1608 found 413.1608.

*5.3.19. 7-(thiophen-2-yl)-2-(3,4,5-trimethoxyphenyl)-[1,2,4] triazolo[1,5-a]pyrimidine (**4s**)*

Yield, 63%; mp: 196.4–197.2 °C; ^{1}H NMR (400 MHz, $CDCl_3$) δ: 3.96 (s, 3H, CH_3O), 4.04 (s, 6H, 2 × CH_3O), 7.37 (t, *J* = 4.4 Hz, 1H, ArH), 7.43 (d, *J* = 4.8 Hz, 1H, ArH), 7.73 (s, 2H, ArH), 7.86 (d, *J* = 5.2 Hz, 1H, ArH), 8.46 (d, *J* = 3.6 Hz, 1H, ArH), 8.76 (d, *J* = 4.8 Hz, 1H, ArH). ^{13}C NMR (100 MHz, $CDCl_3$) δ: 165.38, 156.89, 153.42, 153.15, 141.01, 140.36, 133.71, 132.39, 130.72, 128.23, 125.66, 105.17, 104.84, 60.93, 56.28. HRMS (ESI) *m/z*: calcd for $C_{18}H_{16}N_4O_3S$ (M + H^+) 369.1016 found 369.1017.

*5.3.20. 7-Pyridin-3-yl-2-(3,4,5-trimethoxy-phenyl)-[1,2,4]triazolo [1,5-a]pyrimidine (**4t**)*

Yield, 55%; mp: 235.8–236.2 °C; ^{1}H NMR (400 MHz, $CDCl_3$) δ: 3.93 (s, 3H, CH_3O), 3.98 (s, 6H, 2 × CH_3O), 7.25 (d, *J* = 3.6 Hz,1H, ArH), 7.62 (s, 3H, ArH), 8.60 (d, *J* = 7.6 Hz, 1H, ArH), 8.87 (s, 2H, ArH), 9.42 (s, 1H, ArH). ^{13}C NMR (100 MHz, $CDCl_3$) δ: 165.86, 157.01, 153.99, 153.44, 152.34, 149.81, 144.70, 140.45, 136.72, 126.23, 125.39, 123.48, 108.75, 104.80, 60.90, 56.30. HRMS (ESI) *m/z*: calcd for $C_{19}H_{17}N_5O_3$ (M + H^+) 364.1404 found 364.1404.

*5.3.21. 3-[2-(3,4,5-Trimethoxy-phenyl)-[1,2,4]triazolo[1,5-a] pyrimidin-7-yl]-chromen-2-one (**4u**)*

Yield, 63%; mp: 219.1–219.5 °C; ^{1}H NMR (400 MHz, $CDCl_3$) δ: 3.94 (s, 3H, CH_3O), 3.98 (s, 6H, 2 × CH_3O), 7.48 (t, *J* = 8.0 Hz, 2H, ArH), 7.61 (s, 2H, ArH), 7.74 (d, *J* = 8.0 Hz, 2H, ArH), 7.86 (d, *J* = 4.0 Hz, 1H, ArH), 8.87 (d, *J* = 4.0 Hz, 1H, ArH), 9.39 (s, 1H, ArH). ^{13}C NMR (100 MHz, $CDCl_3$) δ: 165.26, 157.96, 156.90, 154.20, 153.92, 153.43, 147.74, 140.49, 140.44, 134.36, 129.49, 125.42, 125.35, 118.22, 116.92, 116.42, 111.07, 104.79, 60.91, 56.28. HRMS (ESI) *m/z*: calcd for $C_{23}H_{18}N_4O_5$ (M + H^+) 431.1350 found 431.1347.

*5.3.22. 2-(3,4-dichlorophenyl)-7-(3,4,5-trimethoxyphenyl)-[1,2,4] triazolo[1,5-a]pyrimidine (**5a**)*

Yield, 59%; mp: 204.2–205.0 °C; ^{1}H NMR (400 MHz, $CDCl_3$) δ: 3.82 (s, 3H, CH_3O), 3.93 (s, 6H, 2 × CH_3O), 7.68 (s, 2H, ArH), 7.74 (d, *J* = 4.8 Hz, 1H, ArH), 7.83 (d, *J* = 8.4 Hz,1H, ArH), 8.16 (dd, J_1 = 1.6 Hz, J_2 = 8.4 Hz, 1H, ArH), 8.32 (d, *J* = 1.6 Hz, 1H, ArH), 8.93 (d, *J* = 4.4 Hz, 1H, ArH). ^{13}C NMR (100 MHz, $CDCl_3$) δ: 162.32, 157.15, 155.61, 153.17, 147.20, 133.74, 132.30, 131.97, 131.31, 128.79, 127.23, 124.74, 110.26, 107.95, 99.93, 60.67, 56.64. HRMS (ESI) *m/z*: calcd for $C_{20}H_{16}Cl_2N_4O_3$ (M + H^+) 431.0672 found 431.0670.

*5.3.23. 2-(4-methoxyphenyl)-7-(3,4,5-trimethoxyphenyl)-[1,2,4] triazolo[1,5-a]pyrimidine (**5b**)*

Yield, 56%; mp: 194.0–194.6 °C; ^{1}H NMR (400 MHz, DMSO-d_6) δ: 3.80 (s, 3H, CH_3O),3.85 (s, 3H, CH_3O), 3.94 (s, 6H, 2 × CH_3O), 7.13 (d, *J* = 8.8 Hz,2H, ArH), 7.70 (d, *J* = 4.4 Hz, 1H, ArH), 7.73 (s, 2H, ArH), 8.20 (d, *J* = 9.2 Hz, 2H, ArH), 8.88 (d, *J* = 4.8 Hz, 1H, ArH). ^{13}C NMR (100 MHz, DMSO-d_6) δ: 164.53, 161.69, 157.22, 154.79, 153.14, 146.75, 140.78, 128.92, 125.01, 123.14, 114.87, 109.53, 107.91, 60.66, 56.64, 55.74. HRMS (ESI) *m/z*: calcd for $C_{21}H_{20}N_4O_4$ (M + H^+) 393.1558 found 393.1557.

*5.3.24. 2-(p-tolyl)-7-(3,4,5-trimethoxyphenyl)-[1,2,4]triazolo[1,5-a]pyrimidine (**5c**)*

Yield, 58%; mp: 221.0–221.2 °C; ^{1}H NMR (400 MHz, $CDCl_3$) δ: 2.45 (s, 3H, CH_3), 4.01 (s, 9H, 3 × CH_3O), 7.21 (d, *J* = 4.8 Hz, 1H, ArH), 7.33 (d, *J* = 8.0 Hz, 2H, ArH), 7.57 (s, 2H, ArH), 8.28 (d, *J* = 8.0 Hz, 2H, ArH), 8.80 (d, *J* = 4.4 Hz, 1H, ArH). ^{13}C NMR (100 MHz, $CDCl_3$) δ: 165.78, 157.32, 153.65, 153.27, 147.20, 141.25, 140.89, 129.40, 127.63, 127.39, 124.70, 108.14, 107.14, 61.01, 56.41, 21.50. HRMS (ESI) *m/z*: calcd for $C_{21}H_{20}N_4O_3$ (M + H^+) 377.1607 found 377.1609.

*5.3.25. 2-methoxy-5-(7-(3,4,5-trimethoxyphenyl)-[1,2,4]triazolo [1,5-a]pyrimidin-2-yl)aniline(**5d**)*

Yield, 60%; mp: 227.2–228.0 °C; ^{1}H NMR (400 MHz, DMSO-d_6) δ: 3.82 (s, 3H, CH_3O), 3.85 (s, 3H, CH_3O), 3.94 (s, 6H, 2 × CH_3O), 5.00 (s, 2H, NH_2), 6.96 (d, *J* = 8.4 Hz, 1H, ArH), 7.50 (d, *J* = 8.4 Hz, 1H, ArH), 7.58 (d, *J* = 1.6 Hz, 1H, ArH), 7.65 (d, *J* = 4.4 Hz, 1H, ArH), 7.71 (s, 2H, ArH), 8.85 (d, *J* = 4.8 Hz, 1H, ArH). ^{13}C NMR (100 MHz, DMSO-d_6) δ: 165.31, 157.15, 154.53, 153.13, 148.88, 146.65, 140.67, 138.35, 125.14, 123.28, 116.08, 112.32, 110.88, 109.35, 107.84, 60.65, 56.64, 55.80. HRMS (ESI) *m/z*: calcd for $C_{21}H_{21}N_5O_4$ (M + H^+) 408.1667 found 408.1667.

*5.3.26. 2-methoxy-5-(7-(3,4,5-trimethoxyphenyl)-[1,2,4]triazolo [1,5-a]pyrimidin-2-yl)phenol(**5e**)*

Yield, 66%; mp: 177.0–177.6 °C; ^{1}H NMR (400 MHz, DMSO-d_6) δ: 3.82 (s, 3H, CH_3O), 3.85 (s, 3H, CH_3O), 3.91 (s, 6H, 2 × CH_3O), 7.09 (d, *J* = 8.4 Hz, 1H, ArH), 7.68 (d, *J* = 4.8 Hz, 1H, ArH), 7.70 (s, 1H, ArH), 7.72 (s, 3H, ArH), 8.87 (d, *J* = 4.8 Hz, 1H, ArH), 9.40 (s, 1H, OH). ^{13}C NMR (100 MHz, DMSO-d_6) δ: 164.71, 157.18, 154.70, 153.13, 150.41, 147.14, 146.70, 140.74, 125.06, 123.30, 119.05, 114.13, 112.70, 109.45, 107.90, 60.66, 56.64, 56.00. HRMS (ESI) *m/z*: calcd for $C_{21}H_{20}N_4O_5$ (M + H^+) 409.1507 found 409.1504.

*5.3.27. N-(2-methoxy-5-(7-(3,4,5-trimethoxyphenyl)-[1,2,4] triazolo[1,5-a]pyrimidin-2-yl)phenyl) acetamide (**5f**).* Yield, 63%; mp: 236.8–237.2 °C; ^{1}H NMR (400 MHz, DMSO-d_6) δ: 2.15 (s, 3H, CH_3), 3.82 (s, 3H, CH_3O), 3.93 (s, 3H, CH_3O), 3.96 (s, 6H, 2 × CH_3O), 7.22 (d, *J* = 8.4 Hz, 1H, ArH), 7.73 (d, *J* = 4.8 Hz, 1H, ArH), 7.79 (s, 2H, ArH), 7.98 (dd, J_1 = 1.6 Hz, J_2 = 8.4 Hz, 1H, ArH), 8.88 (d, *J* = 4.8 Hz, 1H, ArH), 9.02 (s, 1H, ArH), 9.25 (s, 1H, NH). ^{13}C NMR (100 MHz, DMSO-d_6) δ: 169.12, 164.62, 157.27, 154.75, 153.14, 151.55, 146.57, 140.80, 128.30, 124.89, 123.55, 122.78, 120.30, 111.70, 109.34, 107.88, 60.66, 56.64, 56.33, 24.41. HRMS (ESI) *m/z*: calcd for $C_{23}H_{23}N_5O_5$ (M + H^+) 450.1772 found 450.1772.

5.4. Biological evaluation

5.4.1. Antiproliferative activity

HeLa, A549, HCT-116, and HepG2 cell lines were grown at 37 °C in a CO_2 incubator, in RPMI-1640 or DMEM medium supplemented with 10% fetal bovine serum. Exponentially growing cells were plated in 96-well plates with the density of 2 × 10^3 cells per well and were incubated for attachment at 37 °C for 24 h. Subsequently, culture medium was changed, and cells were treated with tested compounds, DMSO (0.1%) and CA-4, and incubated at 37 °C for 48 h. 20 μL of MTT solution (5 mg/mL) was then added into per well, and plates were incubated at 37 °C for a further 4 h. Then reduced MTT crystals were dissolved, and absorbance was determined by a microplate reader at 570 nm. Finally, the growth inhibitory effects

were represented as IC_{50} values which were calculated with the prism statistical package.

5.4.2. Flow cytometric analysis for cell cycle distribution

2×10^5 Human cervical cancer cells (HeLa) were treated with indicated concentrations (30, 60, 120 nM) of **5e** and the control for 24 h. Subsequently, treated cells were collected, washed with PBS, and fixed by ice-cold ethanol (75%) at 4 °C overnight. Cells were then washed, treated using RNase (50 μg/mL) for 30 min at 37 °C, and stained with propidium iodide. Cell cycle distribution was finally analyzed with flow cytometry (Beckman Coulter).

5.4.3. Apoptosis assay

After treatment with different concentrations of 5e and vehicle for 24 h, cells were collected and incubated using 5 μL Annexin-V/FITC in binding buffer (containing 140 mM NaCl, 10 mM HEPES, 2.5 mM $CaCl_2$, pH 7.4) and 10 μL PI solution for 15 min. Thereafter, the solution was put in the medium and incubated for extra 10 min. Apoptosis was analyzed by FlowJo 7.6 software.

5.4.4. Western blot assays

HeLa cells were homogenized using lysis buffer, after being treated by the process of cell cycle analysis. The protein concentrations were determined using a BSA-100 protein quantitative analysis kit (Biocolor Bioscience & technology, Shanghai, China). Cell lyses were then boiled at 100 °C for 5 min for SDS-polyacrylamide gel electrophoresis (PAGE), after being added the loading buffer. Thereafter, proteins (40μg) were transferred into polyvinylidene fluoride (PVDF) membrane, which was blocked by 5% skim milk at room temperature for 1 h, and then incubated overnight at 4 °C using suitable dilution of primary antibodies, such as β-actin, GAPDH, p-cdc2, cyclin B1, Bax and cleaved PARP. Subsequently, the membrane was washed by TBST/TBS four times, 10 min each time, and incubated with the secondary antibody (1: 4000) at room temperature for 2 h. Finally, the blots were washed in TBST/TBS three times, and the antibody-reactive were revealed by enhanced chemiluminescence (ECL) and exposed on Kodak radiographic film. The images of western blotting were analyzed with Image J (National Institute of Health, Bethesda, United States) program, and statistical analyses were performed using GraphPad Prism version 7.0 (GraphPad Software, La Jolla, CA, United States) software.

5.4.5. Tubulin polymerization assay

The purified tubulin polymerization kit was purchased from Cytoskeleton Inc. (Denver, USA), and experimental details for tubulin polymerization assay were reported in our previous work [29]. PEM buffer (100 μL) containing 2 mg/mL tubulin, 100 mM piperazine-N,N′-bis(2-ethanesulfonic acid) sequisodium salt PIPES (pH 6.9), 1 mM $MgCl_2$, 1 mM EGTA, and 5% glycerol, were pre-incubated in the presence of tested compounds or DMSO on ice. 3 mg/mL concentration of PEG-containing GTP was then added into the mixtures. After 0.5 h, absorbance at 340 nm was calculated with light scattering by a SPECTRA MAX 190 (MD) spectrophotometer every 1 min for 20 min at 37 °C. Plateau absorbance values were used for calculations, and IC_{50} was represented as a sample concentration inhibiting polymerization by 50% after 20 min.

5.4.6. Molecular docking studies

Docking was performed using the representative co-crystallized strucure of tubulin with CA-4 (PDB: 5lyj), and protein structure was prepared using SYBYL 7.3 package [39]. The ligand was extracted and hydrogen atoms were inserted into the crystal. Partial atomic charges were generated to biopolymer with AMBER7 FF99 force field and energy minimization was obtained by the Tripos force field by a distance−dependent dielectric and powell gradient algorithm using a convergence criterion of 0.005 kcal/mol/Å). The surflex module was employed in the docking studies, and all other related parameters were kept at default.

Declaration of competing interest

The authors declare that they have no known competing financial interests or personal relationships that could have appeared to influence the work reported in this paper.

Acknowledgments

This work was supported by grants from the Natural Science Foundation of Guangdong Province, China (Grant No. 2018B030311067), and the Science and Technology Program of Guangzhou City, China (Grant No. 201707010198).

Appendix A. Supplementary data

Supplementary data to this article can be found online at https://doi.org/10.1016/j.ejmech.2021.113449.

References

[1] S. Honore, E. Pasquier, D. Braguer, Understanding microtubule dynamics for improved cancer therapy, Cell. Mol. Life Sci. 62 (2005) 3039−3056.
[2] V. Spanò, R. Rocca, M. Barreca, D. Giallombardo, A. Montalbano, A. Carbone, M.V. Raimondi, E. Gaudio, R. Bortolozzi, R. Bai, P. Tassone, S. Alcaro, E. Hamel, G. Viola, F. Bertoni, P. Barraja, Pyrrolo[2',3':3,4]cyclohepta[1,2-*d*][1,2]oxazoles, a new class of antimitotic agents active against multiple malignant cell types, J. Med. Chem. 63 (2020) 12023−12042.
[3] S. Pecnard, O. Provot, H. Levaique, J. Bignon, L. Askenatzis, F. Saller, D. Borgel, S. Michallet, M.C. Laisne, L. Lafanechère, M. Alami, A. Hamze, Cyclic bridged analogs of isoCA-4: design, synthesis and biological evaluation, Eur. J. Med. Chem. 209 (2020), 112873.
[4] P. Oliva, R. Romagnoli, S. Manfredini, A. Brancale, S. Ferla, E. Hamel, R. Ronca, F. Maccarinelli, A. Giacomini, F. Rruga, E. Mariotto, G. Viola, R. Bortolozzi, Design, synthesis, in vitro and in vivo biological evaluation of 2-amino-3-aroylbenzo[*b*]furan derivatives as highly potent tubulin polymerization inhibitors, Eur. J. Med. Chem. 200 (2020), 112448.
[5] S. Sana, R. Tokala, D.M. Bajaj, N. Nagesh, K.K. Bokara, G. Kiranmai, U.J. Lakshmi, S. Vadlamani, V. Talla, N. Shankaraiah, Design and synthesis of substituted dihydropyrimidinone derivatives as cytotoxic and tubulin polymerization inhibitors, Bioorg. Chem. 103 (2020), 103317.
[6] S.K. Coulup, G.I. Georg, Revisiting microtubule targeting agents: α-Tubulin and the pironetin binding site as unexplored targets for cancer therapeutics, Bioorg. Med. Chem. Lett 29 (2019) 1865−1873.
[7] Y. Luo, Y. Zhou, Y. Song, G. Chen, Y.X. Wang, Y. Tian, W.W. Fan, Y.S. Yang, T. Cheng, H.L. Zhu, Optimization of substituted cinnamic acyl sulfonamide derivatives as tubulin polymerization inhibitors with anticancer activity, Bioorg. Med. Chem. Lett 28 (2018) 3634−3638.
[8] V.S. Dofe, A.P. Sarkate, S.V. Tiwari, D.K. Lokwani, K.S. Karnik, I.A. Kale, S. Dodamani, S.S. Jalalpure, P.V.L.S. Burra, Ultrasound assisted synthesis of tetrazole based pyrazolines and isoxazolines as potent anticancer agents *via* inhibition of tubulin polymerization, Bioorg. Med. Chem. Lett (30) (2020), 127592.
[9] K. Donthiboina, P. Anchi, S. Gurram, G.M. Sai, U.J. Lakshmi, C. Godugu, N. Shankaraiah, A. Kamal, Synthesis and biological evaluation of substituted *N*-(2-(*1H*-benzo[*d*]imidazole-2-yl)phenyl)cinnamides as tubulin polymerization inhibitors, Bioorg. Chem. 103 (2020), 104191.
[10] F. Naaz, M.R. Haider, S. Shafi, M.S. Yar, Anti-tubulin agents of natural origin: targeting taxol, vinca, and colchicine binding domains, Eur. J. Med. Chem. 171 (2019) 310−331.
[11] C.M. Lin, H.H. Ho, G.R. Pettit, E. Hamel, Antimitotic natural products combretastatin A-4 and combretastatin A-2: studies on the mechanism of their inhibition of the binding of colchicine to tubulin, Biochemistry 28 (1989) 6984−6991.
[12] M. Zweifel, G.C. Jayson, N.S. Reed, R. Osborne, B. Hassan, J. Ledermann, G. Shreeves, L. Poupard, S.P. Lu, J. Balkissoon, D.J. Chaplin, G.J.S. Rustin, Phase II trial of combretastatin A4 phosphate, carboplatin, and paclitaxel in patients with platinum resistant ovarian cancer, Ann. Oncol. 22 (2011) 2036−2041.
[13] D.M. Chase, D.J. Chaplin, B.J. Monk, The development and use of vascular targeted therapy in ovarian cancer, Gynecol. Oncol. 145 (2017) 393−406.
[14] V. Spanò, M. Pennati, B. Parrino, A. Carbone, A. Montalbano, A. Lopergolo, V. Zuco, D. Cominetti, P. Diana, G. Cirrincione, N. Zaffaroni, P. Barraja, [1,2]Oxazolo[5,4-*e*]isoindoles as promising tubulin polymerization inhibitors, Eur.

J. Med. Chem. 124 (2016) 840–851.
[15] S.D. Guggilapu, L. Guntuku, T.S. Reddy, A. Nagarsenkar, D.K. Sigalapalli, V.G.M. Naidu, S.K. Bhargava, N.B. Bathini, Synthesis of C5-tethered indolyl-3-glyoxylamide derivatives as tubulin polymerization inhibitors, Eur. J. Med. Chem. 138 (2017) 83–89.
[16] D.A. Ranjan, V. Kumar, H. Kaur, N. Kumar, Y.R. Prakash, R. Poduri, S. Baranwal, V. Kumar, Anti-proliferative potential of triphenyl substituted pyrimidines against MDA-MB-231, HCT-116 and HT-29 cancer cell lines, Bioorg. Med. Chem. Lett 30 (2020), 127468.
[17] V. Spanò, M. Barreca, R. Rocca, R. Bortolozzi, R. Bai, A. Carbone, M.V. Raimondi, A.P. Piccionello, A. Montalbano, S. Alcaro, E. Hamel, G. Viola, P. Barraja, Insight on [1,3]thiazolo[4,5-*e*]isoindoles as tubulin polymerization inhibitors, Eur. J. Med. Chem. 212 (2021), 113122.
[18] V. Spanò, M. Pennati, B. Parrino, A. Carbone, A. Montalbano, V. Cilibrasi, V. Zuco, A. Lopergolo, D. Cominetti, P. Diana, G. Cirrincione, P. Barraja, N. Zaffaroni, Preclinical activity of new [1,2]oxazolo[5,4-*e*]isoindole derivatives in diffuse malignant peritoneal mesothelioma, J. Med. Chem. 59 (2016) 7223–7238.
[19] M. Gilandoust, K.B. Harsha, C.D. Mohan, A.R. Raquib, S. Rangappa, V. Pandey, P.E. Lobie, K.S. Basappa, Rangappa, Synthesis, characterization and cytotoxicity studies of 1,2,3-triazoles and 1,2,4-triazolo [1,5-*a*]pyrimidines in human breast cancer cells, Bioorg. Med. Chem. Lett 28 (2018) 2314–2319.
[20] K. Oukoloff, J. Kovalevich, A.S. Cornec, Y.M. Yao, Z.A. Owyang, M. James, J.Q. Trojanowski, V.M.Y. Lee, A.B. Smith, K.R. Brunden, C. Ballatore, Design, synthesis and evaluation of photoactivatable derivatives of microtubule (MT)-active [1,2,4]triazolo[1,5-*a*]pyrimidines, Bioorg. Med. Chem. Lett 28 (2018) 2180–2183.
[21] Y. Luo, S. Zhang, Z.J. Liu, W. Chen, J. Fu, Q.F. Zeng, H.L. Zhu, Synthesis and antimicrobical evaluation of a novel class of 1,3,4-thiadiazole: derivatives bearing 1,2,4-triazolo[1,5-*a*] pyrimidine moiety, Eur. J. Med. Chem. 64 (2013) 54–61.
[22] B. Huang, C. Li, W. Chen, T. Liu, et al., Fused heterocycles bearing bridgehead nitrogen as potent HIV-1 NNRTIs. Part 3: optimization of [1,2,4]triazolo[1,5-*a*] pyrimidine core *via* structure-based and physicochemical property-driven approaches, Eur. J. Med. Chem. 92 (2015) 754–765.
[23] Y.C. Liu, R.Y. Qu, Q. Chen, J.F. Yang, C.W. N, Z. Xi, G.F. Yang, Triazolopyrimidines as a new herbicidal lead for combating weed resistance associated with acetohydroxyacid synthase mutation, J. Agric. Food Chem. 64 (2016) 4845–4857.
[24] C.N. Chen, Q. Chen, Y.C. Liu, X.L. Zhu, C.W. Niu, Z. Xi, G.F. Yang, Syntheses and herbicidal activity of new triazolopyrimidine-2-sulfonamides as acetohydroxyacid synthase inhibitor, Bioorg. Med. Chem. 18 (2010) 4897–4904.
[25] C.N. Chen, L.L. Lv, F.Q. Ji, Q. Chen, H. Xu, C.W. Niu, Z. Xi, G.F. Yang, Design and synthesis of *N*-2,6-difluorophenyl-5-methoxyl-1,2,4-triazolo[1,5-*a*]-pyrimidine-2-sulfonamide as acetohydroxy acid synthase inhibitor, Bioorg. Med. Chem. 17 (2009) 3011–3017.
[26] F.Q. Ji, C.W. Niu, C.N. Chen, Q. Chen, G.F. Yang, Z. Xi, C.G. Zhan, Computational design and discovery of conformationally flexible inhibitors of acetohydroxyacid synthase to overcome drug resistance associated with the W586L mutation, ChemMedChem 3 (2008) 1203–1206.
[27] Q. Chen, X.L. Zhu, L.L. Jiang, Z.M. Liu, G.F. Yang, Synthesis, antifungal activity and CoMFA analysis of novel 1,2,4-triazolo[1,5-*a*]pyrimidine derivatives, Eur. J. Med. Chem. 43 (2008) 595–603.
[28] F. Yang, L.Z. Yu, P.C. Diao, X.E. Jian, M.F. Zhou, C.S. Jiang, W.W. You, W.F. Ma, P.L. Zhao, Novel[1,2,4]triazolo[1,5-*a*]pyrimidine derivatives as potent antitubulin agents: design, multicomponent synthesis and antiproliferative activities, Bioorg. Chem. 92 (2019), 103260.
[29] B. Zhang, Y.H. Li, Y. Liu, Y.R. Chen, E.S. Pan, W.W. You, P.L. Zhao, Design, synthesis and biological evaluation of novel 1,2,4-triazolo[3,4-*b*][1,3,4]thiadiazines bearing furan and thiophene nucleus, Eur. J. Med. Chem. 103 (2015) 335–342.
[30] X.E. Jian, F. Yang, C.S. Jiang, W.W. You, P.L. Zhao, Synthesis and biological evaluation of novel pyrazolo[3,4-*b*]pyridines as cis-restricted combretastatin A-4 analogues, Bioorg. Med. Chem. Lett 30 (2020), 127025.
[31] W.F. Ma, P. Chen, X.S. Huo, Y.F. Ma, Y. Li, P.C. Diao, F. Yang, S.Q. Zheng, M.J. Hu, W.W. You, P.L. Zhao, Development of triazolothiadiazine derivatives as highly potent tubulin polymerization inhibitors: structure-activity relationship, in vitro and in vivo study, Eur. J. Med. Chem. 208 (2020), 112847.
[32] Q. Li, X.E. Jian, Z.R. Chen, L. Chen, X.S. Huo, Z.H. Li, W.W. You, J.J. Rao, P.L. Zhao, Synthesis and biological evaluation of benzofuran-based 3,4,5-trimethoxybenzamide derivatives as novel tubulin polymerization inhibitors, Bioorg. Chem. 102 (2020), 104076.
[33] F. Yang, X.E. Jian, P.C. Diao, X.S. Huo, W.W. You, P.L. Zhao, Synthesis, and biological evaluation of 3,6-diaryl-[1,2,4]triazolo[4,3-*a*]pyridine analogues as new potent tubulin polymerization inhibitors, Eur. J. Med. Chem. 204 (2020), 112625.
[34] H.A.M. El-Sherief, B.G.M. Youssif, S.N.A. Bukhari, M. Abdel-Aziz, H.M. Abdel-Rahman, Novel 1,2,4-triazole derivatives as potential anticancer agents: design, synthesis, molecular docking and mechanistic studies, Bioorg. Chem. 76 (2018) 314–325.
[35] S.K. Prajapti, A. Nagarsenkar, S.D. Guggilapu, K.K. Gupta, L. Allakonda, M.K. Jeengar, V.G.M. Naidu, B.N. Babu, Synthesis and biological evaluation of oxindole linked indolyl-pyrimidine derivatives as potential cytotoxic agents, Bioorg. Med. Chem. Lett 26 (2016) 3024–3028.
[36] A. Nocentini, D. Moi, A. Deplano, S.M. Osman, Z.A. AlOthman, G. Balboni, C.T. Supuran, V. Onnis, Sulfonamide/sulfamate switch with a series of piperazinylureido derivatives: synthesis, kinetic and in silico evaluation as carbonic anhydrase isoforms I, II, IV, and IX inhibitors, Eur. J. Med. Chem. 186 (2020), 111896.
[37] Y.N. Liu, J.J. Wang, Y.T. Ji, G.D. Zhao, L.Q. Tang, C.M. Zhang, X.L. Guo, Z.P. Liu, Design, synthesis, and biological evaluation of 1-methyl-1,4-dihydroindeno [1,2-*c*] pyrazole analogues as potential anticancer agents targeting tubulin colchicine binding site, J. Med. Chem. 59 (2016) 5341–5355.
[38] C. Da, N. Telang, K. Hall, E. Kluball, P. Barelli, K. Finzel, X. Jia, J.T. Gupton, S.L. Mooberry, G.E. Kellogg, Developing novel C-4 analogues of pyrrole-based antitubulin agents: weak but critical hydrogen bonding in the colchicine site, Med. Chem. Comm. 4 (2013) 417–421.
[39] Sybyl 7.3, Tripos Inc., 1699 South Hanley Road, St. Louis, MO 63144, U.S.A.